To the Graduate Council:

I am submitting herewith a thesis written by James Reed Stanley entitled "Desorption Kinetics of Selected Polynuclear Aromatic Hydrocarbons From Anthropogenically and Artificially Contaminated Soils." I have examined the final copy of this thesis for form and content and recommend that it be accepted in partial fulfillment of the requirements for the degree Master of Science, with a major in Environmental Engineering.

Chris D. Cox

Dr. Chris D. Cox, Major Professor

We have read this thesis and recommend its acceptance:

Kevin G. Robinson

Mriganka M. Ghosh

Accepted for the Council:

Carolyn Minkel

Associate Vice Chancellor
and Dean of the Graduate School

STATEMENT OF PERMISSION TO USE

In presenting this thesis in partial fulfillment of the requirements for a Master's degree at The University of Tennessee, Knoxville, I agree that the Library shall make it available to borrowers under rules of the Library. Brief quotations from this thesis are allowable without special permission, provided that accurate acknowledgment of the source is made.

Permission for extensive quotation from or reproduction of this thesis may be granted by my major professor, or in his absence, by the Head of Interlibrary Services when, in the opinion of either, the proposed use of the material is for scholarly purposes. Any copying or use of the material in this thesis for financial gain shall not be allowed without my written permission.

Signature James Reed Stanley

Date 21 Aug 94

DESORPTION KINETICS OF SELECTED POLYNUCLEAR AROMATIC HYDROCARBONS FROM ANTHROPOGENICALLY AND ARTIFICIALLY CONTAMINATED SOILS

A Thesis

Presented for the

Master of Science

Degree

The University of Tennessee, Knoxville

James Reed Stanley

December 1994

Dedicated to my parents...

Acknowledgements

I would like to express my great appreciation to Dr. Chris Cox. His advice, encouragement, and friendship were invaluable during the times when research seemed overwhelming. I would also like to thank my committee members Dr. Mriganka Ghosh and Dr. Kevin Robinson for their support and interest in this research. Also, I would like to thank Dr. Gary Sayler and Waste Management Research Education Institute for laboratory use and funding.

I would like to thank those people who supported my work in the laboratory. Foremost, to Dr. John Sanseverino for his continual willingness to provide analytical and experimental advice. Also, thanks to Janeen Thonnard, Mike Tschantz, IckTae Yeom, Wally Hunt, Ray Stapleton, Matt Shoesmith, Janice Branson, and Helen Smith.

Finally, I would like to thank my parents and family for their love and support.

Abstract

Experiments were conducted to determine desorption rates of selected PAHs from anthropogenically and artificially contaminated soils. A gas purge apparatus was used to initiate desorption of the sorbed compounds to the aqueous phase and to transfer them to the gas phase. Traps placed in the gas stream were sampled to determine desorption as a function of time. Desorption was less than 15 % over a period of one month for anthropogenically contaminated soils, and ranged from 100 to 79 % in two weeks for soils contaminated artificially and incubated for short time periods. It was concluded that desorption rate was strongly related to contamination age and to the extent of contamination. Ideal reversibility was not apparent which supported the theory of hysteresis.

TABLE OF CONTENTS

CHAPTER		PAGE
1.	INTRODUCTION	1
	1.1 Objectives	4
	1.2 Scope	4
2.	LITERATURE SURVEY	6
	2.1 Adsorption	7
	2.1.1 Adsorption Equilibrium	8
	2.1.2 Adsorbate Mass Transfer-Adsorption Rate	14
	2.2 Desorption	24
	2.2.1 Apparent Equilibrium and Hysteresis	27
	2.2.2 Adsorbate Mass Transfer-Desorption Rate	31
	2.3 Necessity for Future Work	35
3.	MATERIALS AND METHODS	37
	3.1 Soils	37
	3.1.1 Soils Characterization	38
	3.1.2 Soxhlet Extractions	40
	3.2 Artificial Soil Contamination	41
	3.3 Gas Purge Experiments	43
	3.3.1 Gas Purge Apparatus	43
	3.3.2 Tenax Trap Preparation and Extraction	46
	3.3.3 Solution Purge Experiments	48
	3.3.4 Soil Purge Experiments	50
	3.3.5 Residual Soil Extractions	55
	3.4 Analytical	56
	3.4.1 High Pressure Liquid Chromatography	56
	3.4.2 Liquid Scintillation Counting	58
4.	RESULTS AND DISCUSSION	60
	4.1 Soil Characterizations	60
	4.2 Gas Purge Studies	67
	4.2.1 Solution Purge Experiments	68
	4.2.2 Artificially Contaminated Soils	78
	4.2.3 Anthropogenically Contaminated Soils	88
5.	CONCLUSIONS	104
REFERENCES		108
Appendix		113
VITA		116

LIST OF FIGURES

FIGURES		PAGE
3.1	Gas Purge Apparatus	44
4.1	ART Soil Particle Size Distribution	61
4.2	GRI Soil Particle Size Distribution	62
4.3	TN Soil Particle Size Distribution	63
4.4	PAH Removals From Solution During Gas Purge as a Function of Time for Experiment SP200	70
4.5	PAH Removals From Solution During Gas Purge as a Function of Time for Experiment SP400	71
4.6	Determination of Solution-To-Air Mass Transfer Rate Constants for Experiment SP200	74
4.7	Determination of Solution-To-Air Mass Transfer Rate Constants for Experiment SP400	75
4.8	Phenanthrene Removal as a Function of Time in the ART Experiments	80
4.9	PAH Fraction Desorbed as a Function of the Square-Root of Time in the ART Experiments	84
4.10	Phenanthrene Removal as a Function of Time in the ARTGRI Experiment	86
4.11	Phenanthrene Removal as a Function of the Square-Root of Time in the ARTGRI Experiment	87
4.12	PAH Removals as a Function of Time in the GRI Experiment	90
4.13	PAH Removal as a Function of The Square-Root of Time in the GRI Experiment	91
4.14	Removal of Phenanthrene as a Function of Time in the ARTGRI and GRI Experiments	94
4.15	PAH Removals as a Function of Time in the TN Experiment	96
4.16	PAH Removals as a Function of the Square-Root of Time in the TN Experiments	97

4.17 PAH Removals as a Function of Time in the TNCLDN2 Experiment 99

4.18 PAH Removals as a Function of the Square-Root of Time in the TNCLDN2 Experiment 100

A.1 Chromatogram for PAH Standards 114

A.2 Chromatogram for PAH Extraction from Soil 114

LIST OF TABLES

TABLE		PAGE
3.1	Summary of Solution Purge Experimental Parameters	49
3.2	Experimental Parameters for Desorption Experiments with Laboratory Contaminated Soils	52
3.3	Experimental Parameters for Desorption Experiments with Anthropogenically Contaminated Soils	54
4.1	Particle density, carbon content, and total aerobic heterotrophs of soils	64
4.2	Soxhlet Extraction Data for TN and GRI Soils	66
4.3	Summary of Experimental Recoveries	72
4.4	Rate and Henry's Constants Summary	77
4.5	Solubility Data for PAHs of Interest	93
4.6	Summary of Desorption Rate Data	102

Chapter 1

INTRODUCTION

Polycyclic aromatic hydrocarbons (PAHs) constitute a major class of pollutants found at former manufactured gas plants (MGPs) and wood-treating facilities (WTFs) (Lane and Loehr, 1992). Manufactured gas plants operated in the United States from the early 1800's until the mid-1950's, and produced gas from coal and oil in order to satisfy the growing demand for electricity (ERT Project, 1984). The waste by-products from this process typically consisted of sludges, tars, spent oxide waste and ash materials. These wastes were usually disposed of on-site or sold to other industries as raw material. In particular, the wood treatment industry refined coal-tar waste to creosote and applied it directly to wood surfaces as a preservation treatment. Creosote was typically used as a pesticide (Mueller et al., 1989). Approximately 500 WTFs currently consume 454,000 metric tons of creosote annually. Numerous contaminated sites exist today as a result of improper handling of coal tar at MGPs and creosote at WTFs including: misuse, accidental spillage, improper disposal, leaking tanks, drippings without effective catchment, and leachate from unlined holding ponds (ERT Report, 1984; Mueller et

al., 1989).

PAHs, phenolics, light aromatics, inorganic sulfur, nitrogen species, and trace metals constitute the major classes of chemicals in MGP waste (ERT Project, 1984). Specifically, PAHs, which are further classified as hydrophobic organic compounds (HOCs), constitute a large fraction of priority pollutants found in the waste. Mueller et al. (1989) report that coal tar creosote contains 85 % PAHs. PAH compounds found in coal tar and creosote are characterized by low aqueous solubility, high adsorption affinity, persistence in the environment, carcinogenicity, and biodegradability (ERT Project, 1984).

The manner in which PAH contaminants desorb from soil to the aqueous phase is important because PAH transformation and transport are aqueous-phase dependent (Lane and Loehr, 1992). Many remediation technologies are also dependent on this transfer, including: bioremediation, pump-and-treat, air sparging, and soil-vapor extraction (Mueller et al., 1989; Farrell and Reinhard, 1994a). Therefore, quantitating the rate at which a pollutant adsorbs and desorbs from soil is of particular importance for understanding and modeling pollutant fate and transport in natural soil systems (Karickhoff, 1981). Various sorbent/sorbate systems have been studied in recent years to quantitatively characterize

sorption kinetics for specific compounds so that informed decisions regarding management and eventual remediation of sites can be made. Past investigations of HOC sorption have shown that there are characteristic ways in which organic compounds sorb and desorb in soil systems and that related compounds may follow similar trends (Oliver, 1985; Lane and Loehr, 1992). However, actual kinetics of sorption is compound-specific and can vary significantly among related compounds. Therefore, in order to accurately describe a given system, compound-specific data is required.

Adsorption has been more extensively studied than desorption, and it remains unclear as to the kinetic equivalence of adsorption and desorption for a particular compound (Kan et al., 1994). Sorption mechanisms have been characterized in the past for numerous artificially constructed sorbent/sorbate systems in laboratory settings maintained at ideal conditions. However, little work has been performed to investigate how compounds desorb from anthropogenically contaminated soils in natural systems, especially for long contamination ages (e.g. MGP and WTF sites). Anthropogenically contaminated soils are especially difficult to study because they are heterogeneous, highly weathered, and contaminated by pollutant mixtures of unknown quantity and distribution within soil grains. The obvious need for compound-specific desorption data for soils which

have been anthropogenically contaminated with PAHs serves as the motivation for this study.

1.1 Objectives

The main objective of this research is to determine desorption kinetics for selected PAHs from two separate anthropogenically contaminated soils. Desorption kinetics as a function of contamination age from an artificially contaminated soil is measured for comparison.

1.2 Scope

Accurate fate and transport modeling of PAHs in natural systems is dependent on the availability of applicable experimental data. Experiments and methods were designed to yield insight into the kinetics of PAH desorption from soil. Initially, the soil was characterized and the mass-transfer characteristics of the apparatus were determined. Experiments were then performed on two anthropogenically contaminated soils and one artificially contaminated soil to quantify the rate of desorption for selected PAHs. To initiate continuous non-equilibrium desorption of PAHs, a purge and trap system, consisting of a gas source, hydration and purge flasks, and a synthetic trapping agent were utilized. Desorption kinetics of selected PAHs were

determined from analysis of the experimental data.

Chapter 2

LITERATURE SURVEY

Sorption theory and knowledge have evolved from the basic desire to understand the manner in which a sorbent affects a solute. In the past, adsorption has been thoroughly studied and characterized due in part to the potential for use in water/wastewater treatment. The need to understand both forward and reverse sorption processes (adsorption and desorption) in soil and groundwater systems has recently moved to the forefront of research interest. This is attributed to the overwhelming number of contaminated sites located throughout the United States and elsewhere. A better understanding of sorption mechanisms and kinetics in soil/contaminant systems is requisite in understanding fate and transport processes, and for modeling, waste management, and remediation applications. To this end, research goals are being oriented to further characterize sorption processes in natural systems.

2.1 Adsorption

Adsorption has been defined as the uptake of a solute (or adsorbate) by an adsorbent (Benefield et al., 1982). In other words, over a finite period of time, a solute is removed from solution by an adsorbent material which has an affinity for the solute. Initially, solute molecules transfer through a film of solvent surrounding adsorbent particles and diffuse into the pores of the particle. The majority of solute molecules become attached to adsorbent pore surfaces by chemical or physical adsorption. In chemical adsorption, a chemical reaction creates a bond between adsorbate and adsorbent. In physical adsorption, van der Waal's or electrostatic forces hold the solute to the adsorbent surface. The majority of adsorption processes occur by a combination of both physical and chemical mechanisms.

Adsorption fundamentals have been studied extensively in water and wastewater treatment. Adsorption theory has been established in large part from these studies and subsequently related to many different sorbate/sorbent systems. For example, adsorption theories developed to describe water and wastewater treatment processes have been extended to describe contaminated soil systems (Wu and Gschwend, 1986; Oliver, 1985; Pavlostathis and Jaigal,

1991). Previous agronomy research has greatly aided in the application of fundamental sorption theory to natural soil systems (Karickhoff, 1981). Basic concepts developed from the study of pesticide sorption and can be applied to other contaminants as well. Adsorption theory provides an understanding of the characteristics of a sorbate/sorbent system at equilibrium, and the rate at which a system approaches equilibrium.

2.1.1 Adsorption Equilibrium

Partitioning of organic compounds between the soil and aqueous phases can be conceptualized as follows:

$$C_W \rightleftharpoons C_S \qquad 2.1$$

In a closed system at equilibrium, the concentrations of the organic compound in the water phase, C_W, and on the solid phase, C_S, remain constant. For an adsorbate and an adsorbent in a closed system, equilibrium refers to a steady-state condition with respect to adsorbate concentration in the water and soil phases (Karickhoff and Morris, 1985). Karickhoff defines equilibrium as a thermodynamic condition in which sorbed and solution compound fugacities are the same, with fugacity defined as escaping tendency (Karickhoff, 1981). Alternatively, equilibrium can be defined as the equivalence of chemical

potentials in both phases (Lee, 1992a).

Different system conditions can be defined and studied experimentally in a laboratory setting. Adsorption data can yield insight into equilibrium sorption distribution of the adsorbate between solvent and adsorbent. Information obtained from these experiments can then be expressed graphically using adsorption isotherms.

The Langmuir, Freundlich, Brunaur-Emmett-Teller (BET), and equilibrium partitioning isotherms are commonly used to describe adsorption distribution (Benefield et al., 1982; Oliver, 1985). The Langmuir, Freundlich, and equilibrium partitioning isotherms are frequently used in analysis of soils contaminated with organic pollutants, therefore, they will be described in detail.

The Langmuir isotherm is derived from studies in monolayer gas adsorption on homogeneous surfaces (Farrell and Reinhard, 1994a), and is expressed mathematically as:

$$q = \frac{q_o b C_w}{(1 + b C_w)} \qquad 2.2$$

where:

q = adsorbed concentration

b = Langmuir coefficient

C_w = adsorbate aqueous concentration

q_o = monolayer adsorption capacity

The Langmuir equation is based on several assumptions (Benefield et al., 1982): (1) the adsorption is monolayer, (2) equal adsorption affinity at each adsorption site, and (3) adjacent adsorbed molecules do not affect adsorption of one another.

The Freundlich isotherm is empirical in nature and has found wide-spread usage for describing adsorption of mixed solutes and dilute solutions (Benefield et al., 1982). The underlying assumptions of this isotherm are: (1) a heterogeneous adsorbent surface, (2) different adsorption site classes, and (3) adsorption on each site class following a Langmuir relationship. The Freundlich isotherm was originally developed for monolayer gas sorption on heterogeneous solids (Farrell1 and Reinhard, 1994a):

$$q = K_F C_w^{1/n} \qquad 2.3$$

where:

q = adsorbed concentration

K_F = Freundlich coefficient

C_w = adsorbate aqueous concentration

n = Freundlich exponent

Equilibrium adsorption of organic compounds in soil and sediment has been studied by many researchers (Oliver, 1985; Wu and Gschwend, 1986; DiToro and Horzempa, 1982; Means et al., 1980). For a system of known adsorbent and contaminant mass, the equilibrium partitioning of nonpolar organics to sediment can often be characterized by assuming a linear adsorption isotherm as follows (Oliver, 1985):

$$K_p = C_s / C_w \qquad 2.4$$

where:

K_p = adsorption partition coefficient

C_s = contaminant concentration on sediment

C_w = contaminant concentration in water

This equation represents the equilibrium partitioning of a contaminant to sediment.

Several parameters of adsorbent/adsorbate systems have been investigated to explain the adsorption process. Experiments have shown that K_p depends strongly on suspended solids concentration (Oliver, 1985). Oliver states that microparticulate suspended solids that may remain in solution after the solid-liquid separation process can contribute to experimental artifact. It has also been noted

that adsorption of some organic compounds to soil can be directly correlated with the organic carbon content or organic matter content of a sediment (Farrell and Reinhard, 1994a; Lane and Loehr, 1992; Karickhoff, 1981; Connaughton et al., 1993). Karickhoff (1981) states that adsorption can be correlated directly to organic content of the adsorbent, with K_p related to the fraction of organic carbon present in an adsorbent. With this consideration, researchers have further characterized the adsorption process by normalizing the adsorption partition coefficient for the organic carbon content of a sediment (Oliver, 1985).

$$K_{oc}=K_p/f_{oc} \qquad 2.5$$

where:

K_{oc} = partition coefficient normalized for carbon

K_p = adsorption partition coefficient

f_{oc} = organic carbon fraction of the soil

More recently it has been noted that the composition of the organic carbon can affect the adsorption behavior of nonpolar compounds (Murphy et al., 1990)

An alternative and indirect means of calculating K_{oc} from a compounds octanol/water distribution coefficient, K_{ow}, is described by Karickhoff (1981) and is shown in the following equation:

$$K_{oc} = \frac{\theta^{o}}{\theta^{oc}} K_{ow} \qquad 2.6$$

where:

K_{oc} = partition coefficient normalized for carbon

K_{ow} = octanol/water partition coefficient

Θ^{o} = solute in octanol fugacity coefficient

Θ^{oc} = solute bound to soil fugacity coefficient

It has been demonstrated that equilibrium adsorption of organic chemicals to soil can follow both linear and non-linear adsorption isotherms (Karickhoff, 1981; Young and Ball, 1994; Farrell and Reinhard, 1994a). Equation 2.4 is commonly used to model linear adsorption. In experiments where sorption does not follow a linear trend, the Langmuir and Freundlich models are frequently used to characterize the process. Non-linear behavior is typically explained by effects produced when high affinity adsorption sites are preferentially filled, or when adsorption approaches a limiting value (Farrell and Reinhard, 1994a).

Miller and Pedit (1992) state that non-linear sorption occurs commonly in natural systems. Therefore, recognizing the occurrence of non-linear behavior is imperative in fate and transport modeling. An important characteristic of non-linear adsorption is discussed by Kan et al. (1994), namely that transport rates can be erroneous if linear models are

used when non-linearity exists. For example, concentration profiles from non-linear adsorption processes exhibit early breakthrough and tailing, compared to those resulting from linear adsorption processes. The mathematics describing non-linear behavior are more difficult than for linear adsorption; therefore, the latter is often assumed for simplicity (e.g. Ball and Young, 1994).

2.1.2 Adsorbate Mass Transfer - Adsorption Rate

The time required for a particular sorbate/sorbent system to approach equilibrium is largely controlled by the mass transfer of an adsorbate in the adsorbent particles (Harmon and Roberts, 1993; Wu and Gschwend, 1986). The aqueous and soil phase concentrations as a function of time can be predicted only by understanding the mass-transfer processes.

Adsorption rates are largely dependant on basic system parameters (Benefield et al., 1982). Mixing, adsorbent particle size, adsorbate solubility, adsorbate size, pH, and temperature are factors which determine the rate at which a particular system reaches equilibrium. Various combinations of these parameters control sorption capacity and kinetics for a given system. For example, mixing can control which sorption mechanism, film or particle diffusion, is rate-

limiting. Adsorption rate increases with increasing surface area (decreasing particle size). In some instances, the rate is proportional to adsorbate solubility (Benefield et al., 1982). Adsorption increases as the size of an adsorbate molecule approaches adsorbent pore size. Various compounds adsorb at higher rates when pH is controlled at an optimum level. This is due to ionization effects and sorbent affinity for hydrogen ions at different pH. Temperature can be correlated to the kinetic energy of an adsorbate molecule and is proportional to sorption rate as well.

It is probable that ideal equilibrium sorption does not occur in natural systems where boundary conditions remain in constant flux and mass transfer of adsorbate is rate-limiting (Wu and Gschwend, 1986; Miller and Pedit, 1992; Brusseau et al., 1991). According to Wu and Gschwend (1986), in these instances, equilibrium models such as those given in 2.1.1 cannot be used independently to model adsorption in real soils. If a system is not completely isolated and maintained until equilibrium is attained, the mechanisms of nonequilibrium sorption are dominant.

Nonequilibrium can be viewed as a condition in which a system with defined boundaries is not given sufficient time to completely equilibrate due to rate limitations and

changing system parameters. In the past, contaminant advection and dispersion times have been assumed to be significantly greater than sorption and desorpiton times (Miller and Pedit, 1992). Therefore, it has been commonly assumed that local sorption/desorption equilibrium conditions exist. However, Miller and Pedit (1992) state that in some instances sorption may occur so slowly that the previous assumption is invalid.

Brusseau and coworkers (1991) further define non-equilibrium as consisting of two classes: (1) transport-related, and (2) sorption-related nonequilibrium. Transport-related nonequilibrium is associated with heterogeneous flow paths. Sorption-related nonequilibrium is a result of chemical non-equilibrium or rate-limited diffusive mass transfer. Brusseau suggests that chemical nonequilibrium (rate-limited interactions between sorbate and sorbent) is not a probable rate-limiting mechanism for HOC sorption, due to the greater importance of HOC partitioning between solution and organic matter within the sorbent. Rather, diffusive mass-transfer is suggested to be the primary rate-limiting mechanism.

Diffusive mass-transfer can be further defined as being either film diffusion, retarded intraparticle diffusion, or intrasorbent diffusion (Brusseau et al., 1991).

Intraorganic matter diffusion is defined as adsorbate diffusion strictly within the adsorbent (organic matter) matrix, and retarded intraparticle diffusion is defined as aqueous-phase diffusion of solute through adsorbent pores with instantaneous equilibrium sorption/desorption occuring along the pore wall. However, Brusseau (1991) states that intraorganic matter diffusion has been suggested to be a form of retarded intraparticle diffusion, and that distinguishing between the two processes is not necessary under operational conditions. The study shows that film diffusion is not an important rate-limiting mechanism for non-ionic, low polarity organics. Retarded intraparticle diffusion and intrasorbent diffusion are proposed to be the major nonequilibrium rate-limiting mechanisms. Miller and Pedit (1992) also state that these two processes are important when considering slow sorption rates resulting in nonequilibrium diffusion.

Diffusion modeling using Fick's laws has been successfully utilized by numerous researchers to explain mass transfer rate behavior of selected organic compounds in contaminated soils under nonequilibrium conditions (Young and Ball, 1994; Harmon and Roberts, 1993; Farrell and Reinhard, 1994b).

$$\frac{\partial S}{\partial t} = D_a \nabla^2 C \qquad 2.7$$

where:

S = adsorbed compound concentration

D_a = apparent diffusion coefficient

C = solute concentration

∇ = directional gradient operator

This equation describes adsorbate concentration and movement as a function of time, and also shows that diffusion is a function of concentration gradient.

The basic approach for diffusion modeling in saturated systems assumes that the effects of surface and film diffusion are minimal, the system is well-mixed, spherical and homogeneous adsorbent particles, and that diffusion is the primary rate-limiting mass-transfer mechanism.

Wu and Gschwend (1986) propose a diffusion model to describe sorption rates of HOCs in natural soils and sediments, which relies on known sorption processes and available descriptive sorbent/sorbate parameters. The retarted intra-particle diffusion model specifically assumes radial penetration of adsorbate into adsorbent, that the entire surface area of adsorbent is available for mass flux, and that the diffusion path length is the particle radius. A similar model is given by Young and Ball (1994), but the rate of mass transfer is controlled by both retarded intra-

particle and intra-sorbent diffusion. Young and Ball (1994) applied this approach for modeling the transport of TCE through aquifer material.

The diffusion process of an adsorbate into an adsorbent particle is given in the following equation, as given by Young and Ball (1994), using Fick's law and a mass balance over a volume element.

$$\epsilon_i \frac{\partial C_{im}}{\partial t} + \rho_a \frac{\partial q}{\partial t} = \frac{\epsilon_i}{r^2} \frac{\partial}{\partial r} [r^2 D_p \frac{\partial C_{im}}{\partial r}] + \frac{\rho_a}{r^2} \frac{\partial}{\partial r} [r^2 D_s \frac{\partial q}{\partial r}] \quad 2.8$$

where:

C_{im} = solute mass in pore water at time t and radius r / volume of pore water

q = solute mass adsorbed to intraparticle solid at time t and radius r/mass sorbent

ε_i = intraparticle porosity

ρ_a = apparent density

D_p = effective pore diffusion coefficient

D_s = effective adsorbed-phase diffusion

t = time

r = radial distance in adsorbent

This equation expresses the diffusion rate of compound as a function of adsorbent radius and unit volume. Equation 2.8 shows that diffusion occurs as a result of concentration

gradient. This gradient is the difference in contaminant concentration between the soil-bound phase and the aqueous phase. The model can be further simplified if local equilibrium is assumed in the interstitial adsorbent pores and that local partitioning can be described linearly as follows:

$$q = K_d C_{im} \qquad 2.9$$

where:

q = solid phase concentration

K_p = equilibrium partitioning coefficient

C_{im} = intrasorbent fluid concentration

In other words, as a solute molecule diffuses radially through adsorbent pores, it is constantly partitioning between the adsorbed and desorbed phases. If equation 2.9 accurately describes this partitioning and diffusion coefficients are constant, the model can be expressed as follows:

$$\frac{\partial C_{im}}{\partial t} = \frac{D_a}{r^2} \frac{\partial}{\partial r} \left[r^2 \frac{\partial C_{im}}{\partial r} \right] \qquad 2.10$$

where:

C_{im} = intrasorbent fluid concentration

D_a = apparent diffusion coefficient

t = time

r = adsorbent particle radius

The apparent diffusion coefficient can be further defined as a term which combines the effects of the effective pore diffusion, D_p, and the effective sorbed-phase diffusion, D_s, and is defined as follows:

$$D_a = \frac{\epsilon_i D_p}{(\epsilon_i + \rho_a K_d)} + \frac{\rho_a K_d D_s}{(\epsilon_i + \rho_a K_d)} \qquad 2.11$$

where:

D_a = apparent diffusion coefficient

ϵ_i = intraparticle porosity

D_p = effective pore diffusion coefficient

D_s = effective sorbed-phase diffusion

ρ_a = apparent density

K_p = equilibrium linear partitioning coefficient

The experimentally measured apparent diffusion coefficient does not differentiate between pore and sorbed-phase diffusion, and therefore cannot be used to discriminate between the two adsorption mechanisms. It reflects the overall process of diffusion through pores and through the adsorbent phase.

If diffusion through adsorbed phase can be neglected, D_a can be simplified as follows:

$$D_a = \frac{D_p}{1 + \frac{\rho_a K_d}{\epsilon_i}} \qquad 2.12$$

where:

D_a = apparent diffusion coefficient

D_p = effective pore diffusion coefficient

ρ_a = apparent density

K_p = equilibrium linear partitioning coefficient

ε_i = intraparticle porosity

In this case D_a is inversely proportional to K_d, which means that the approach to equilibrium decreases with increasing hydrophobicity. On the other hand, in the case where aqueous diffusion can be neglected, D_a can be written as follows:

$$D_a = \frac{D_s}{\epsilon/\rho_a K_d + 1} \qquad 2.13$$

where:

D_a = apparent diffusion coefficient

D_s = effective sorbed-phase diffusion

ε_i = intraparticle porosity

ρ_a = apparent density

K_d = equilibrium linear partitioning coefficient

If this relationship is used and adsorbed-phase diffusion presides, D_a is not dependent on concentration or K_d for hydrophobic organic compounds where $\varepsilon_i/\rho_a K_d << 1$.

Young and Ball (1994) further state that non-linearity

may exist in systems characterized by a wide range of solute concentrations. In this case, a Freundlich isotherm is proposed in place of Equation 2.9 with K_d defined as follows:

$$K_d = \frac{q}{C} = K_f C^{(1/n)-1} \qquad 2.14$$

where:

K_p = equilibrium partitioning coefficient

q = solid-phase concentration

C = solute concentration in the aqueous phase

K_f = Freundlich coefficient

1/n = Freundlich exponent

Modeling diffusion using Fick's Law presents many complexities, however. Some of these have been identified by Farrell and Reinhard (1994b) and include: (1) the accuracy of pore characterization with an average D_e, (2) extrapolating experimental results performed for small concentration ranges can be erroneous, because desorptive capability may be concentration dependant and cloak true sorption mechanisms, and (3) the assumption of instantaneous equilibrium. Detailed soil characterizations and a priori non-equilibrium knowledge are required for Fick's diffusion to be applicable, whereas this information is not required in other models (e.g. first order mass transfer). Despite the complexities, it is probable that only mechanistic

models (e.g. Fick's) will provide fundamental sorption information and be applicable in a wide range of systems.

Other simplified models have been described to model sorption in real soils (Wu and Gschwend, 1986; Karickhoff and Morris, 1985; Breauseau et al., 1990). This is, in part, due to the desire to simplify the modeling process associated with using diffusion modeling. The most simple model used is termed the one-box model. In this model, a single rate constant quantifies sorption as related to concentration difference between solution and sorbent. A second model which typically fits experimental data more closely is referred to as a two-compartment model and divides sorption into easily accessible sites and slowly exchanging sites. A disadvantage of the two-compartment model is that three separate fitting parameters are required, whereas some diffusion models require only one fitting parameter.

2.2 Desorption

Desorption can be defined as partitioning of adsorbate from the adsorbent into a solvent. In essence, desorption is the reverse of adsorption. For example, contaminated sediment can become resuspended and slowly desorb compounds into overlying water, or run-off water flowing through

vadose zone regions can desorb pollutants from contaminated soils and transfer them to groundwater systems. Desorption is analogous to adsorption in may ways and will be discussed in detail.

Guidelines have been postulated in an effort to generalize the desorption process for different adsorbent/adsorbate systems based on common parameters such as: (1) adsorbate solubility, (2) adsorbent carbon content, (3) adsorbent particle size, (4) residence time or contamination age of compound on soil, and (5) adsorbent porosity, As mentioned previously, the partitioning of an adsorbate to an adsorbent has been correlated to adsorbate solubility (Lee et al., 1992b; Karickhoff, 1981; Oliver, 1985). The generalization of compound solubility relating to desorption from anthropogenically-contaminated soils has met with limited success (Pavlostathis and Mathavan, 1992). Correlations between K_d and compound octanol/water partitioning, K_{ow}, have shown excellent agreement (Lee et al., 1992a). This type of simple partitioning has been related to transfer of PAH's from diesel fuel into water, K_{dw}, and can be directly correlated with a compounds K_{ow}.

As described earlier, the carbon content of an adsorbent is proportional to adsorptive capacity. Also, as particle size deceases, surface area increases

proportionally. Pavlostathis and Mathavan (1992) have demonstrated that contamination age or residence time of an organic compound bound to soil strongly affects desorption characteristics for four separate volatile organic compounds (VOCs). The study found that the mass fraction of compound resistant to desorption increases with increasing residence time; however, it did not conclusively establish direct correlations between residence time trends and general system characteristics (e.g. organic carbon content, surface area). Porosity has been studied and characterized in three categories (Farrell and Reinhard, 1994a). Macropores are greater than 500 A, mesopores are 20 to 500 A, and micropores or slits are less than 20 A. Several sorption characteristics have been found to be related to pore diameter. For example, soils having only mesopores show no capillary effect, while particles with a large fraction of micropores exhibit a strong tendancy to adsorb organic molecules. Also, chemicals are desorbed faster with increasing temperature according to Oliver (Oliver, 1985).

Despite documented non-consistencies, solubility remains an important issue in sorption partitioning for PAHs (Lee et al., 1992a; Lee et al., 1992b). Lee (1992a) has formulated an expression, based on Raoult's law, to predict the partitioning behavior of chemicals in an organic phase to an aqueous phase. The equilibrium mole fraction of a

compound in the organic phase is directly proportional to aqueous concentration. The relationship between K_d and aqueous solubility is given by:

$$\log K_d = -\log S_1 - \log(MW_o/\rho_o) \qquad 2.15$$

where:

K_d = liquid-liquid partition coefficient

S_1 = aqueous solubility of the liquid solute

MW_o = constituent average molecular weight

ρ_o = constituent average density

In Lee's studies, equation 2.15 is successfully used to predict PAH partitioning between water and diesel fuel. A similar equation is then used to predict the release of coal-tar-bound PAHs to water. Due to the complexity of coal tar relative to diesel fuel, deviations from ideal behavior are expected; however, model predictions and experimental results typically agreed within a factor of 2.

2.2.1 Apparent Equilibrium and Hysteresis

The general definition of equilibrium has been established previously in section 2.1.1. With respect to desorption, equilibrium retains the same meaning. For example, desorption of contaminant from the soil in contact with water in a closed system occurs until equilibrium is established. At equilibrium, the concentrations of

adsorbate in the adsorbent and aqueous phases remain constant. The amount of time required for equilibrium desorption to occur varies greatly with system conditions.

Equilibrium desorption can be conceptualized using equation 2.16 and is analogous to the forward process described earlier.

$$K_D = C_s / C_w \qquad 2.16$$

where:

K_D = desorption partition coefficient

C_S = contaminant concentration on sediment

C_W = contaminant concentration in water

Typically, batch experiments are performed to characterize K_D (DiToro and Horzempa, 1982; Means et al., 1980; Pavlostathis and Jaigal, 1991). In these experiments, fresh water is added to a known mass of contaminated soil with a known loading of contaminant. The suspension is mixed in order to facilitate compound desorption to the aqueous phase. Desorption is allowed to continue until apparent equilibrium is reached. The aqueous concentration is measured to determine desorbed mass and K_D can then be calculated.

In the past, it has been common practice to equilibrate a sediment/contaminant mixture for approximately 24 hr for

sorption measurement. Lane and Loehr (1992) have shown that apparent equilibrium is reached in this time frame for adsorption of PAH's. However, the question of desorption equilibrium remains and it is presently unclear as to when true equilibrium conditions are obtained in many systems. Kan et al. (1994) states that an adsorbent material may not exhibit equivalent adsorption and desorption characteristics. Thus the questions of equilibrium and reversibility surface.

Apparent equilibrium can be defined as constant aqueous solute concentration within a sorbate/sorbent system. The term "apparent" is used in many instances to denote the fact that even though solution concentration may be changing at a rate too small to detect, the concentration within soil particles may be changing, as a function of adsorbent particle radius (Karickhoff and Morris, 1985). This diffusion within individual particles establishes non-equilibrium conditions, but is not readily apparent by measuring aqueous-phase concentration. As described earlier, the question of true system equilibrium is currently being discussed by many researchers. As previously stated, the question of complete sorption reversibility has been investigated by numerous researchers. DiToro and Horzempa (1982) state that reversibility is not complete for PCB153, and that desorption partition

coefficients were much higher than adsorption partition coefficients.

Adsorption/desorption hysteresis is the general term referring to the occurance of different isotherms for adsorption and desorption processes in a given contaminant/soil system (Kan et al., 1994; DiToro and Horzempa, 1982; Miller and Pedit, 1992). Miller and Pedit (1992) list possible explanations for the experimental observance of hysteresis as follows: (1) solute degradation or loss, (2) slow desorption rate, (3) solute sorbing to non-settling particles, (4) competing solutes, (5) changing sorbent characteristics, and (6) site-specific bonding. Obtaining different adsorption and desorption isotherms for the same compound contradicts ideal behavior, which predicts instantaneous equilibrium, isotherm linearity and desorption reversibility. However, hysteresis is not always evident in sorption systems as reported by Karickhoff (1981). In Karickhoff's study, sorption isotherms were generated for neutral hydrophobic compounds which exhibit linearity and reversibility, for low loading limits.

Hysteresis has been reported for many organic compounds, including PAH's (Kan et al., 1994). In the past, hysteresis has been attributed to initiation of desorption before equilibrium is reached, resulting in an apparently

slow desorption rate. The results of Kan's study show that for PAHs contaminated with soils for a period of a few days, the time required to fully desorb the compounds may be on the order of years. This is a strong basis for suggesting that there is a fraction of PAH which may be extremely resistant to desorption or irreversibly bound. The occurrence of hysteresis has also been suggested to be a result of experimental artifact (DiToro and Horzempa, 1982). However, experiments were performed to verify the existence of hysteresis by changing experimental conditions for the same sorption systems and noting the effects. Analysis of experimental data shows that changing experimental conditions did not show experimental artifact and that hysteresis remains.

2.2.2 Adsorbate Mass Transfer - Desorption Rate

Soils and sediments which have been anthropogenically contaminated with organic compounds can be a continual source of pollution due to mass-transfer limited desorption of the pollutant (Oliver, 1985). Several investigators have discussed basic trends associated with desorption in natural systems. Pavlostathis and Mathavan (1992) state: "A two-phase pattern of desorption of organic chemicals from soils has been revealed by kinetic studies. An initial fast stage (in hours) and a subsequent longer, slow phase (in days)

have been observed." Karickhoff (1985) and DiToro (1982) have also reported labile and nonlabile desorption characteristics for PAH's and PCB's sorbed on sediment. All have noted a biphasic desorption pattern for soils and sediments contaminated with organic compounds. Incubation time or contamination age has been found to be inversely proportional to the easily desorbed mass fraction (Pavlostathis and Jaigal, 1991; Oliver, 1985). Connaughton et al. (1993) report that naphthalene shows continuously increasing resistance to desorption. Increased steric effects, increased sorption energies, and increased surface area, which result from microporosity, were postulated to cause desorption kinetics to decrease significantly.

Temperature has a significant effect on desorption. "Temperature obviously plays a major role in the desorption process with much faster desorption occurring at higher temperatures" (Oliver, 1985). Harmon and Roberts (1993) also describe the effect of temperature on desorption rates. This study demonstrates that desorption behavior is affected by the temperature at which the sample is initially equilibrated.

Batch experiments are used to characterize sorption equilibrium and mass-transfer rates for numerous sorbent/sorbate systems (Pavlostathis and Jaigal, 1991;

Means et al., 1980; Kan et al., 1994). These studies produce valuable information relating to equilibrium partition coefficients, kinetics, reversibility, hysteresis, and numerous sorption characteristics associated with sorbent or sorbate properties. However, batch studies may not be fully indicative of processes occurring where sorbate/sorbent systems remain in constant flux (Brusseau et al., 1990).

Karickhoff and Morris (1985) have presented an alternate means of characterizing desorptive rate behavior. Infinite depth/planar source modeling has been used to effectively describe desorption in laboratory data. This method is applicable to systems in which a contaminated sediment is suspended in water and continuously purged to remove desorbed contaminant from the aqueous phase. During the initial period of such an experiment, the soil functions as an infinite depth, planar source and desorption behavior can be modeled using the following equation:

$$f_s(t) = k_s t^{1/2} \qquad 2.17$$

where:

$f_s(t)$ = fraction of adsorbate released

k_s = diffusive constant

t = time

In this equation, k_s incorporates structural characteristics

of the adsorbent and the effective diffusion coefficient for the adsorbate. Restrictive boundary conditions limit the applicability of this approach for fate and transport modeling, but it does provide useful analysis of laboratory desorption data in systems where the aqueous concentration of contaminant is minimized.

Recently, diffusion modeling has been proposed to predict sorption behavior in anthropogenic soil systems (Harmon and Roberts, 1993; Farrell and Reinhard 1994b). Dynamic experiments have been used by researchers as an alternative to batch studies (Brusseau et al., 1990; Karickhoff and Morris, 1985). Harmon and Roberts (1993) have noted that for diffusion modeling, external boundary conditions greatly affect mass-transfer rates. A maximum desorption potential is created if a zero-concentration boundary condition is maintained. In fate and transport modeling, this can be viewed as the maximum desorption rate and becomes useful for management decisions.

Several researchers have used gas purge (also referred to as aqueous purge) techniques to achieve zero-concentration boundary conditions (Karickhoff and Morris, 1985; Oliver, 1985; Brusseau et al., 1990). Utilizing this type of apparatus enables the researcher to obtain information relating to maximum non-equilibrium desorption

rate, where adsorbate mass transfer is rate-limiting. A conceptualization of the sorption condition established in gas purge experimentation is as follows:

$$C_g \leftrightarrow C_w \leftrightarrow S \qquad 2.18$$

where:

C_g = compound concentration in gas phase

C_w = compound concentration in aqueous phase

S = sorbed compound concentration

In these experiments contaminated soil is suspended in water and gas is bubbled through it. Desorption of contaminants from the soil to the aqueous phase is initiated by maintaining a zero-concentration boundary condition. Compounds which desorb into the aqueous phase are stripped to the air phase following a Henry's Law relationship (Oliver, 1985). Information obtained can be used to calibrate and validate desorption models and to provide the maximum rate of soil-to-water mass transfer.

2.3 Necessity for Future Work

Predicting the fate and transport of contaminants which are present in natural soil systems is of extreme importance. In order to accomplish this objective, the theory and mechanisms of sorption must be applicable and thoroughly understood. A sorption-rate model coupled with a

transport model, if accurate, can provide such information (Karickhoff, 1981; Young and Ball, 1994). However, information must be obtained relating sorption rates for specific sorbent/sorbate systems to their physical and chemical characteristics. This is necessary to validate fundamental sorption theory and mathematical models. Therefore, there is a tremendous need for data describing the desorption of specific contaminants from natural soil through experimental techniques. More specifically, there are numerous sites which contain huge quantities of soil contaminated with coal tar and creosote residue. Specific information is needed to characterize the process of desorption for priority pollutants found in the residue - primarily PAH's. This will allow waste management, remediation, and modeling decisions to be made more effectively. It is the purpose of this work to investigate the kinetics of desorption of selected PAH's present in anthropogenically contaminated soils taken from MGP and WTF sites.

Chapter 3

MATERIALS AND METHODS

3.1 Soils

Three soils were used in desorption experiments. Two of the soils were heavily contamianted with coal tar and creosote and the other soil was previously uncontaminated. The first anthropogenically contaminated soil was taken from a WTF in Chattanooga, TN in May 1992 (TN soil). The second contaminated soil was taken from New York state at an MGP site and is called the Gas Research Institute soil (GRI). The clean soil was obtained from a region in middle Tennessee and was used for artificial contamination experiments (ART soil). All experiments were conducted using soils that had passed through a sieve (2 mm for ART and TN, 3.5 mm for GRI).

In order to characterize the soils used in desorption experiments, studies were conducted to determine particle size distribution, solid density, carbon content, and total aerobic heterotrophs (TAH). Also, soxhlet extractions were preformed on the anthropogenically contaminated soils to obtain estimates of contaminant loadings.

3.1.1 Soils Characterization

Particle size distribution was obtained by weighing an aliquout of soil and air drying it under a fume hood. Typically, 100 to 150 g of soil was used for this analysis. The sieve trays were previously cleaned and weighed in order to determine, by difference, the weight of soil retained in each tray after the sieve analysis was completed. In all experiments, sieve sizes of 40, 70, 100, and 200 mesh were used for size distribution analysis. The soil was placed in the nest of sieves and then placed on a sieve shaker for 10 minutes. The "fines" were characterized by the "hydrometer method" (Gee and Bauder, 1986). In this method, 40 g of each soil was suspended in 1 L of water contained in a settling column. The suspension was allowed to settle for 1 day while hydrometer measurements were taken at various intervals. Hydrometer measurements were then transformed to particle sizes using equations given in the reference.

Solid density (mass of soil/volume of soil) was determined by weighing approximately 20 g of a soil, which had been air dried, into a 200 mL flask. The flask and soil were then weighed together and recorded. Dry CO_2 was used to purge the flask and soil for several hours to saturate the soil pores. Deionized water, previously degassed by vacuum filtration, was added to the flask and allowed to

equilibrate for approximately one day. Additional water was added to bring the total volume to 200 mL. The flask was reweighed with the volume of solid determined by converting the mass of water to volume and subtracting from the total flask volume.

Soil carbon content was determined by the Plant and Soil Science Department at the University of Tennessee by soil combustion in a Leco CR 12 Carbon System. Before analysis, the soil was pulverized and dried in a dessicator for several days. Analysis was performed in triplicate for each sample by collecting 0.5 g sample aliquots which passed a .019 mm sieve. These samples were placed in the analyzer at 2300 °F. When combustion occured, the free carbon was combined with oxygen to form CO_2, which was then measured and related to the original weight of the sample to give carbon fraction.

Anthropogenically contaminated soils were characterized based on microbial population. For this analysis 1/4 strength yeast-extract peptone glucose (YEPG) ager was prepared and poured into several plates and allowed to cure overnight. 1 g of soil was placed in a centrifuge tube and suspended in 9 mL of sodium pyrophosphate buffer with vortex mixing. Triplicate soil slurries were prepared with triplicate series dilutions taken from each tube. Plates

were innoculated from each dilution series and incubated for a period of four days. The plates were counted to determine the colony forming units/mass of soil. The ager selected for this study was conducive to growth of aerobic heterotrophic microorganisms, typically found in soils.

3.1.2 Soxhlet Extractions

Triplicate soxhlet extractions were used to establish baseline contaminant loadings for each soil. 10 g of an air dried soil was placed in an extraction thimble and the thimble placed in the soxhlet apparatus. Methylene chloride (150 to 200 mL) was added and the system was sealed. The condensor water was turned on and the system was heated in a water bath to approximately 45 °C, or until reflux conditions were established. The system was maintained at these conditions for at least 24 hr. When the extraction period had ended the bath was turned off and the system was allowed to return to room temperature. The condensor was then turned off and removed from the apparatus. Approximately 50 mL of fresh methylene chloride was poured into the thimble compartment and allowed to siphon into the bottom flask for rinsing purposes. Compressed nitrogen was used to evaporate the solvent by attaching the bottom flask to a ring stand and placing a tube from the nitrogen cylinder into the throat of the flask. Nitrogen flow was

maintained until the solvent had completely evaporated (usually on the order of several hours). Acetone (25 to 75 mL) was added to resuspend the residue in the flask bottom. The concentration of fluorene, phenanthrene, and anthracene were determined in the extractant by diluting the acetone into acetonitrile for HPLC analysis.

3.2 Artificial Soil Contamination

Contamination of soils was accomplished by adding a known volume of phenanthrene stock solution to a known mass of soil. The stock solution was prepared by adding excess phenanthrene crystals to autoclaved, deionized water in an erylenmeyer flask. A screw cap lined with aluminum foil was used to seal the flask and prevent vapor-phase phenanthrene from adsorbing to the cap lining. The solution was stirred for approximately one day to allow dissoluiton of phenanthrene. The solution was filtered in a disposable vacuum apparatus with a 0.22 um nylon filter to remove excess particulate phenanthrene. The filtrate was transferred to a clean flask and capped. A small aliquot of the filtrate was collected and analyzed by HPLC to check for solution purity. Radiolabeled ^{14}C phenanthrene was then added to the nonlabeled solution by dissolving the labeled solid in approximately 1.5 mL of methanol and spiking the nonlabeled solution with a glass microsyringe. Solution

activity was checked using LSC after each spike of labeled compound until the desired activity was reached. Typically, the methanol fraction in the final solution was approximatley 0.020 to 0.025 %. Prior to soils contamination, the solution was reanalyzed to determine specific activity and total phenanthrene concentration. Specific activity was measured with LSC, and the total phenanthrene concentration was determined by measurement with HPLC, or by the addition of nonlabeled concentration (HPLC) and labeled concentration (LSC). The indirect method of adding the nonlabeleled and labeled concentrations to determine a total concentration was used in some cases to prevent contamination of the HPLC system.

The ART and GRI soils were used for artificial contamination experiments. Soils were prepared for contamination by weighing approximately 2 g of soil into a weigh boat on an analytical balance and transferring to a 25 mL centrifuge tube. The soil, tube, cap, and septa were autoclaved for 20 minutes three succesive times. The sample was allowed to cool overnight and then autoclaved once more and allowed to cool. Contamination of the soils was accomplished by adding 25 mL of the phenanthrene stock solution to each tube. A small section of aluminum foil was used with the screw cap and septa for sealing each tube. The soils were suspended in the solution with a vortex mixer

for approximately 15 seconds and then placed on a lab rotator at approximately 100 rpm. Soils which had contamination ages less than one week were rotated continuously. Soils contaminated greater than one week were rotated continuously for one week and then stored vertically in a test tube rack with periodic vortex mixing. When a desired contamination age had been reached, the centrifuge tube was centrifuged at 6500 rpm for 35 min., and the supernatant analyzed with LSC. The supernatant analysis was used to determine, by difference, the mass loading on the contaminated soil.

3.3 Gas Purge Experiments

The soils described above are used in conjunction with gas purge techniques to determine the rate of PAH desorption from contaminated soils. This section will describe the experimental apparatus, preparation and extraction of Tenax traps, apparatus characterization experiments, PAH desorption experiments, and residual PAH extractions from soil for mass balance purposes.

3.3.1 Gas Purge Apparatus

Gas purge experiments were conducted with the apparatus shown in Figure 3.1. Air and nitrogen were selected as

Figure 3.1 Gas Purge Apparatus

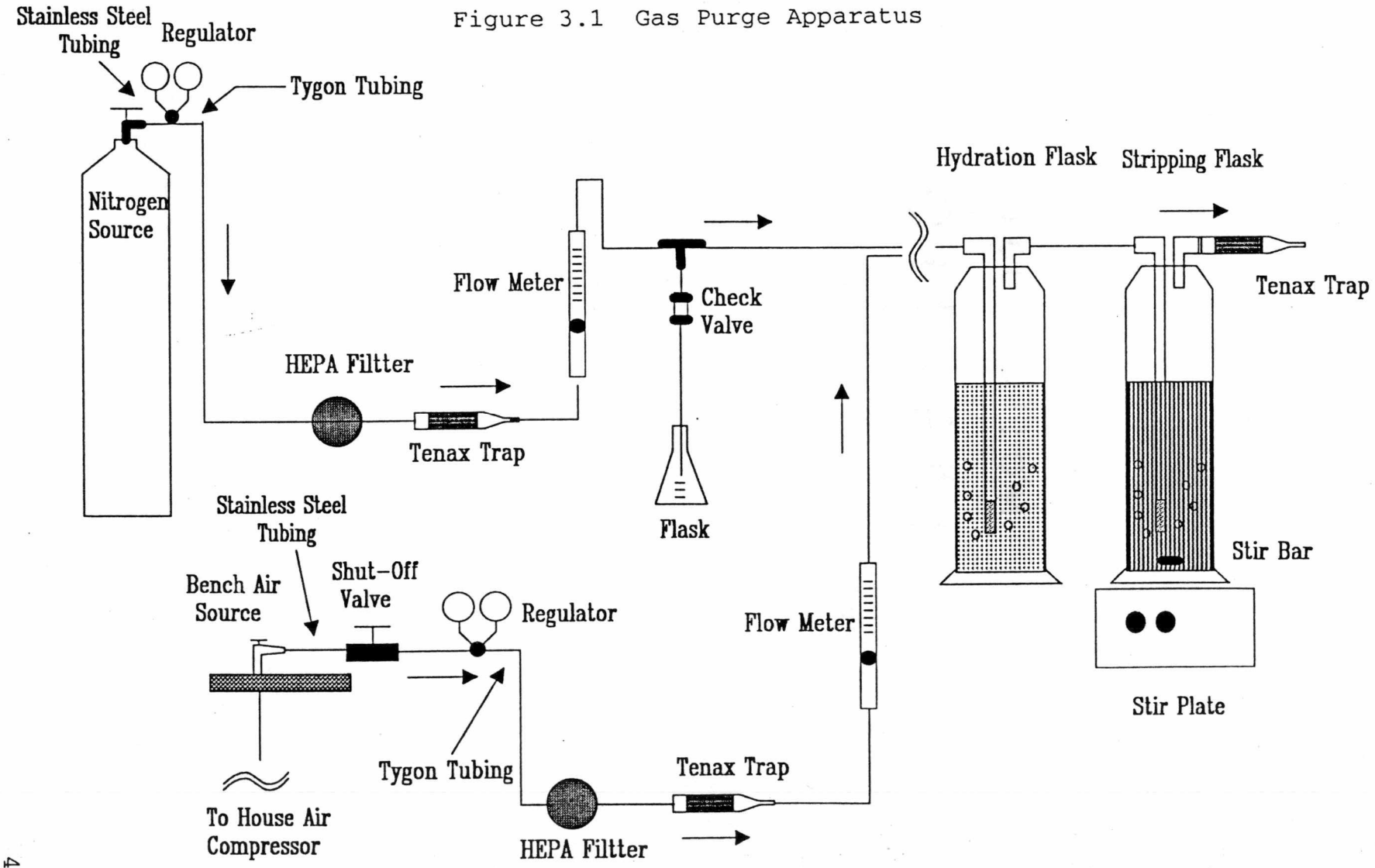

purge gases in the desorption studies. A single gas source was selected and used for each experiment based on desired purging conditions. Initial experiments were conducted with air as the gas source. Later experiments were conducted with nitrogen due to concern over aerobic biodegradation. Air was supplied by an in-house compressor, and the nitrogen was supplied by pressurized cylinders. The air pressure was controlled with a single stage regulator, with the high pressure side of the regulator connected to the bench-top house air outlet with stainless steel tubing and NPT fittings. A shut-off valve was placed in-line before the regulator for control and safety purposes. The nitrogen source was controlled with a two-stage regulator attached directly at the cylinder head. For safety considerations, a 25 psi pressure release valve was placed in-line before the purging flasks for experiments where nitrogen cylinders were used as the gas source.

Tygon tubing was attached to barbed fittings on the low pressure side of the regulators, for both gas source arangements, and used to channel flow through the rest of the apparatus. A 0.3 um HEPA filter and Tenax trap were inserted in the flow stream following the regulators to remove particulate matter and organic contaminants present in the gas stream. The gas flow was quantitated with a rotometer, which was positioned in-line after the first

Tenax trap. In most experiments, the flow controler on the rotometer was kept entirely open, with flow rate controlled by the regulator. This reduced head drop across the rotometer and minimized the pressure gradient across the system, which was maintained at < 10 psi for most experiments.

The gas flow was routed from the flow meter into a 500-mL purge flask for hydration and then into a 250-mL purge flask, where solute stripping occured. A Teflon-coated magnetic stirrer was used to suspend the soil in the stripping flask. Purged organics were trapped in a second Tenax trap, connected to the purge flask by a short section of Tygon tubing. This trap was pushed into the Tygon tubing until the front of the trap became flush with the purge flask effluent tube to minimize contact between tubing and gas. Paraffin was used to prevent system leakage by securely wraping all sections joined by Tygon tubing or ground glass fittings. The system was slightly pressurized and tested for leakage with a soapy-water solution before experiments were conducted.

3.3.2 Tenax Trap Preparation and Extraction

Tenax-TA resin, 60/80 mesh, was used to trap PAHs present in the air phase during all desorption experiments.

A single trap was prepared by packing a small amount of glass wool into the tip of a 5 mm i.d. pasteur pipette. Uniform packing of the Tenax was achieved by tapping the pipette on the bench top between successive small additions of the resin. The volume of resin desired inside a single trap was calculated beforehand and expressed as a length term inside the pipette barrel. The calculated length typically ranged from 2.0 to 3.5 cm and was measured from the glass wool plug in the tip, up the barrel to obtain the approximate volume (2000 mm^3 to 3500 mm^3). A second piece of glass wool was used to hold the resin in the pipette. A small vacuum in the direction of flow was applied to each trap. After several seconds the vacuum was disconnected and the trap repacked to ensure that the resin was evenly distributed throughout the barrel. In some experiments, another glass wool plug was inserted into the end of the barrel to act as a particulate filter during sampling. The traps were prepared in batches and stored vertically on the tips.

When a trap was taken for extraction and analysis, it was scored with a metal file slighlty above the Tenax line in the barrel and on the tip. The pipette was broken in these two positions, and the pipette and contents were transferred to a 25 mL centrifuge tube with Teflon septa. The Tenax resin was removed from the pipette by tapping the

broken barrel on the inside of the centrifuge tube. If the resin could not be freed in this way, the end of a swab was used to push the resin out of the pipette. The swab only came into contact with the glass wool plug during this procedure.

Acetonitrile or hexane was added to each centrifuge tube for extraction of PAH from the resin. Each tube was capped and placed on a lab rotator at approximately 100 rpm overnight. A sample aliquot of supernatant was recovered from an extraction tube by centrifugation. Depending on the availability of analysis instrumentation, the traps were sometimes batched for extraction and analysis. In this case, the tip and barrel of each trap was flame sealed and wrapped with paraffin for storage.

3.3.3 Solution Purge Experiments

For the solution purge experiments, an aqueous solution containing the three PAH's of interest (fluorene, phenanthrene, and anthracene) was prepared and stripped with air in the gas purge apparatus. Specific experimental parameters are summarized in Table 3.1. The efficiency of the experimental procedure and the liquid-gas solute mass-transfer characteristics were obtained. Two solution purge experiments were performed and were titled solution purge

Table 3.1 Summary of Solution Purge Experimental Parameters

Expt. Name	Spike Fl Conc[1] (mg/L)	Spike Ph Conc[1] (mg/L)	Spike An Conc[1] (mg/L)	Gas Source & Flow Rate[2] (mL/ min)	Tenax Trap Extract-ions[3]	Bio-cide dose (mg/L) & Organic phase[4] (%)
SP200	1.525	0.663	0.026	Air	Aceto-nitrile	650
				800	10	0.440
					6000	
					10	
SP400	0.950	0.408	0.024	Air	Aceto-nitrile	650
				800	10	0.275
					5000	
					15	

[1]Concentration of compound in stripping flask initially.
[2]Gas source and flow rate used during experimentation.
[3]Solvent and amount (mL), centrifuge speed (rpm) and time (min).
[4]Biocide dose & solvent present in aqueous solution from spike.

200 (SP200) and solution purge 400 (SP400).

Initially, a 500 mg/L stock solution of each PAH was prepared by weighing solid PAH into a small glass vial. Acetone was added to each vial to dissolve the PAH. The stock solutions were then used to prepare an aqueous solution of the desired concentration of each PAH component. The aqueous concentration of each PAH was typically maintained at 50 to 80 % of the aqueous solubility. Sodium azide was added to the system for supression of biological degradation of the PAH during purging. The aqueous solution was mixed thoroughly and transferred to the stripping flask in the gas-purge apparatus. The apparatus was sealed and a Tenax trap placed in the effluent stream of the stripping flask. The regulator was adjusted to give a desired flow rate. Trap sampling intervals were based on estimation and trial-and-error for these experiments. When the experiment was completed, the solution in the stripping flask was sampled to determine if their was a significant concencration of PAH remaining in solution. Tenax traps were extracted with organic solvent and analyzed with HPLC.

3.3.4 Soil Purge Experiments

Four experiments were conducted with artificially contaminated soils. Specific experimental parameters are

listed in Table 3.2. The ART soil was used in three of the experiments with contamination ages of 2 days, 20 days, and 10 months (ART2d, ART20d, and ART10m) for phenanthrene. The GRI soil was also re-contaminated with phenanthrene for 5 days and stored at 4 °C until desorption experimentation (ARTGRI). In the artificially contaminted soil experiments, the ^{14}C-phenanthrene solution was poured off from the centrifug tube following a desired contamination period and the contamintated soil was transferred to the stripping flask with successive water rinses. Sodium azide was added to the stripping flask as a biocide, and a Teflon-coated stir bar was added to the system to provide continuous mixing. Deionized, sterilized water was then added to bring the total volume within the flask to 200 mL. The gas flow was initiated, with trap sampling at various intervals. When a trap was sampled, the flow was shut-off briefly for a trap to be removed. A new trap was then inserted in the apparatus and the flow was reinitiated. For ^{14}C-labeled experiments, the hydration and stripping flasks were placed in a hood behind an explosion shield for safety considerations. Desorbed compounds were extracted with organic solvent from Tenax traps and measured with LSC.

Two anthropogenically contaminated soils were obtained and characterized for use in the gas purge apparatus for desorption experiments. Three experiments were conducted

Table 3.2 Experimental Parameters for Desorption Experiments with Laboratory Contaminated Soils

Expt Name	Phen on Soil (ug/g) & Age[1]	Gas & Flow[2] (mL/min)	Tenax Trap Extract-ions[3]	Expt Sieve Size[4] (mm)	Bio-cide dose (mg/L) & slurry (%)
ART2d	13	Air	Hexane	2.0	650
	2 day	400	10		1
			6500		
			35		
ART20d	5	Air	Hexane	2.0	650
	20 day	400	10		1
			6500		
			35		
ART10m	10	Air	Hexane	2.0	650
	10 month	400	10		1
			6500		
			35		
ARTGRI	14	Nitrogen	Hexane	3.35	650
	5 day	400	10		1
			6500		
			35		

[1]Phenanthrene loading on soil and contamination age of soil.
[2]Gas source used and flow rate.
[3]Solvent and amount (mL), centrifugation speed(rpm) and time (min).
[4]Experimental sieve size that soil was passed through.
[5]Biocide dosage and fraction of soil slurried in the aqueous phase.

with the anthropogenically contaminated soils. Specific experimental parameters are given in Table 3.3. The first two experiments were conducted with the TN and GRI soils (TN and GRI experiments). The third experiment was conducted with the TN soil at 4 °C with nitrogen as the purge gas (TNCLDN2 experiment). Three contaminant compounds (fluorene, phenanthrene, and anthracene) were studied from each soil. The soils were air dried before use in a fume hood for a period of several days and placed on a balance to verify an equilibrium state was reached (no water loss or gain noticable as a decrease or increase in weight).

Desorption experiments with anthropogenically contaminated soils were conducted by transferring 1 to 2 g of a soil into the stripping flask. Sodium azide was added as a biocide and deionized, autoclaved water was added until the total volume reached 200 mL. The system was sealed, and the gas flow initiated and maintained at a constant flow. The soil was suspended by continuous mixing with a Teflon coated stir bar. Tenax traps were taken and replaced with new traps at various sampling intervals. The traps were either batched for later analysis or analyzed immediately depending on instrument availability. Desorbed compounds were extracted from the traps with organic solvent and analyzed on HPLC.

Table 3.3 Experimental Parameters for Desorption Experiments with Anthropogenically Contaminated Soils

Expt Name	Soxhlet Mass on Soil (ug/g)[1]	Trap Extract-ion[2]	Gas & Flow[3] (mL/min)	Expt Sieve Size[4] (mm)	Biocide Dosage (mg/L) & Slurry[5] (%)
TN	Fl-24	Aceto-nitrile	Air	2.0	650
	Ph-37	10	800		0.5
	An-8	6500			
		35			
GRI	Fl-123	Aceto-nitrile	Air	3.35	650
	Ph-234	10	800		0.5
	An-61	6500			
		30			
TNCLDN2[6]	Fl-24	Aceto-nitrile	Nitrogen	2.0	650
	Ph-37	15	400		1
	An-8	6500			
		35			

[1]Compund loading on soil as determined by soxhlet extractions.
[2]Solvent and volume (mL), centrifuge speed (rpm) and time (min).
[3]Source gas and flow rate used.
[4]Experimental sieve size.
[5]Biocide dosage and fraction of soil in aqueous slurry.
[6]Experiment performed @ 4°C.

3.3.5 Residual Soil Extractions

When a desorption experiments was completed, the soil was rinsed into ten, 25 mL tubes, with rinsing, and centrifuged at 6500 rpm for 35 min. Following centrifugation, the supernatant was poured off and the remaining soil consolidated into a fewer number of tubes with rinsing. This process was repeated until the purged soil was recovered in one tube.

Residual phenanthrene was recovered from artificially contamintad soils by a hexane extraction was as follows: hexane (typically 20 mL) and water (5 mL) were added to the 25 mL centrifuge tube containing the recovered soil for a final recovery extraction of phenanthrene from the soil. This extraction process lasted on the order of 1 day to several weeks with the hexane phase sampled and analyzed with LSC to determine mass recovery.

Recovered anthropogenically contaminated soils were air dried in a fume hood for several days and then extracted in either a soxhlet apparatus, or by using an ether extraction similar to the hexane extraction described above. In most experiments, both extractions were performed on the purged soil. Extractant analysis was performed by diluting the extractant into acetonitrile and mearuring on HPLC.

3.4 Analytical

In all experiments analytical measurements of PAHs were conducted using one of two techniques, high performance liquid chromatography (HPLC), or liquid scintillation counting (LSC). This section will describe the analytical procedures used with each technique for measurement of samples.

3.4.1 High Performance Liquid Chromatography

Sample analysis was conducted with a Waters High Performance Liquid Chromatography (HPLC) system. The system consisted of three model 501 pumps, a WISP model 712 autosampler, a Vydac C_{18} reverse phase column, a model 420 fluoresence detector, a model 486 UV/Vis detector, and a PC with Baseline Logo software. Acetonitrile and water were selected as the diluents for analysis. Standards were typically prepared by serial dilution from an organic-phase stock solution into pure acetonitrile. In some cases a 50:50 acetonitrile/water solution was used for dilution purposes to determine if better peak resolution was obtainable. If the acetonitrile/water solution was used for standard dilution, the samples selected for analysis were also diluted with the same solution. However, in the majority of cases, standards were diluted into 100 %

acetonitrile and samples were extracted and diluted, if necessary, with 100 % acetonitrile. Acetonitrile blanks were typically injected after every third sample to ensure that no residual analyte was retained within the system. In the majority of cases, a four point linear calibration curve was used, with sample response bracketed by high and low standard response. Quantitation was based on peak integration, which was conducted with the integration feature contained in the software. This consisted of defining the beginning and end points of analyte peaks and a chromatogram baseline. This was done by using the automatic feature contained in the software initially and then making fine adjustments to custom fit integration parameters to the peak of interest. In some instances, analyte peaks could not be fully resolved. Subjective judgement was used to define peak beginnings and end points relative to baseline. In these cases integration parameters were manually selected and systematically used for similar samples. For all analyses, a gradient was selected to give maximum resolution of analyte peaks for quantitation. The analysis diluent gradient typically consisted of equilibrating the column for several minutes with acetonitrile and water (50:50) at 1.2 mL/min. Then a linear ramp was used to bring the concentration of acetonitrile to 100 % over 20 minutes. This flow condition was held for 7 minutes and then ramped back to 50 % acetonitrile over 3 minutes. The column was

allowed to equilibrate at 50:50 for five minutes before another sample was analyzed. Standard samples and unknown samples were quantitated with the same gradient. Gradients were obtained based on previous trial-and-error attempts to define optimal gradient parameters for a given sample matrix. Representative standard and sample chromatograms are shown in Appendix A.

3.4.2 Liquid Scintillation Counting

LSC analysis was performed by adding 10 mL of scintillation cocktail (Ready-Safe cocktail for aqueous samples and Econo-fluor cocktail for organic samples) to a glass scintillation vial with aluminum foil-lined cap and then adding 0.1 - 1 mL of sample. In desorption experiments, 0.5 mL or 1 mL samples were typically used, with the amount of sample added depending on the sensitivity required and the available sample volume. The sample vial was then vortex mixed for several seconds and stored overnight in the dark to allow the sample to "settle". Analysis of the sample consisted of selecting a pre-programmed method from the instrument software with an identification card that was placed on the sample rack. The sample rack containing the sample vials was placed in the Beckman liquid scintillation counter and the method was activated. Each sample was counted automatically and the

results were recorded on a strip chart.

Calibrating the instrument for a particular method consisted of selecting a particular scintillation cocktail and matrix which would contain the sample. For example, if the samples were ^{14}C Phenanthrene in water, Ready-Safe cocktail was selected and water was the sample matrix. Then several vials were prepared with 10 mL of cocktail in each and successively increasing volumes of water (e.g. 0.1 mL - 1 mL). An equivalent amount of ^{14}C phenanthrene acitivity was then added to each vial. Each vial was mixed and allowed to settle in the dark before analysis. A quenching curve for the analyte in the sample matrix (water) was then established from the sample analysis. Ideally the instrument would report equal acitvities for all samples, however, the sample matrix produced a quenching effect which affected the "true" activity. When a quench curve was established, it was programmed into the instrument and used for sample analysis.

Chapter 4

RESULTS AND DISCUSSION

4.1 Soil Characterizations

GRI, TN, and ART soils were characterized according to their particle size distribution, particle density, carbon content, and total aerobic heterotrophs (for the GRI and TN soils only). The particle size distributions for the GRI, TN, and ART soils are shown in Figures 4.1, 4.2, and 4.3, respectively. The hydrometer method (Gee and Bauder, 1986) was used to characterize the "fines", and sieving was used for the larger fractions. Particle size distribution is reported as percentage of total mass smaller than the stated particle size. It can be seen that the majority of soil mass is below 500 microns in size for the ART soil. This soil contains the largest fraction of fine particles. The GRI soil displays the opposite trend with the majority of particles being larger than 500 microns. The TN soil exhibits a mid-range trend with approximately 45 % of particles being less than 500 microns. Particle density, organic carbon content, and total aerobic heterotroph counts are reported in Table 4.1. Particle density, ρ_s, refers to the mass of solid per unit volume of solid. Particle

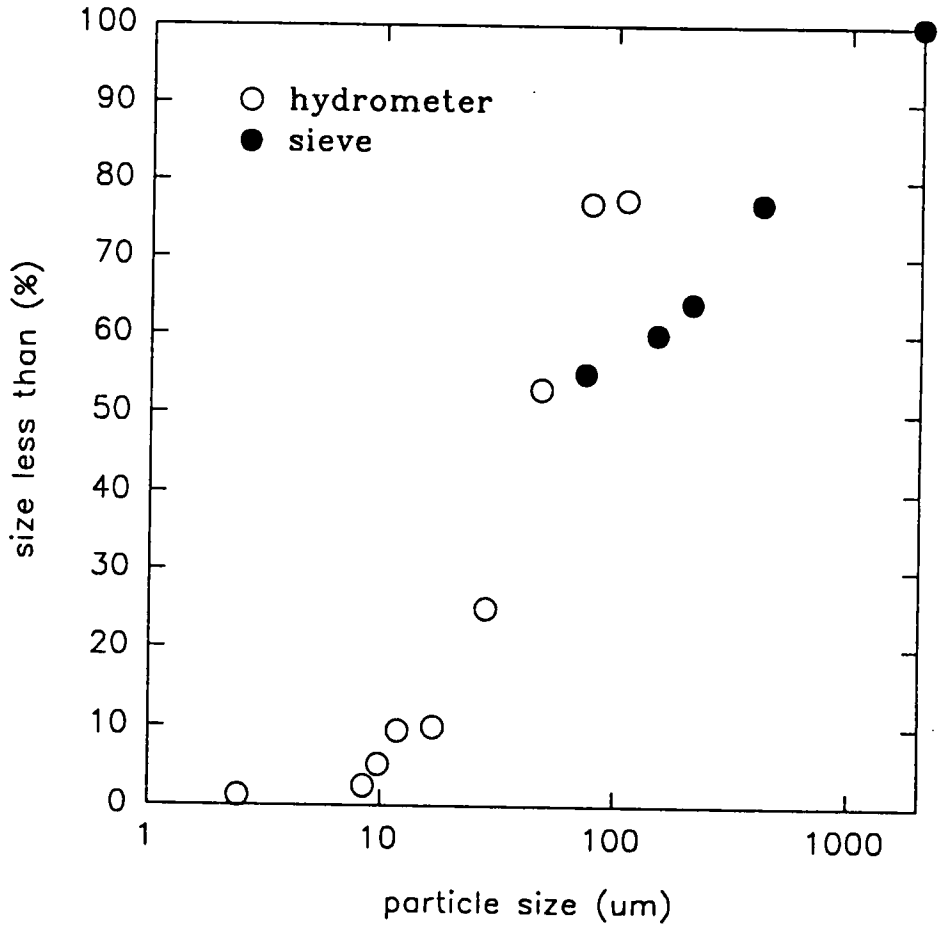

Figure 4.1 ART Soil Particle Size Distribution

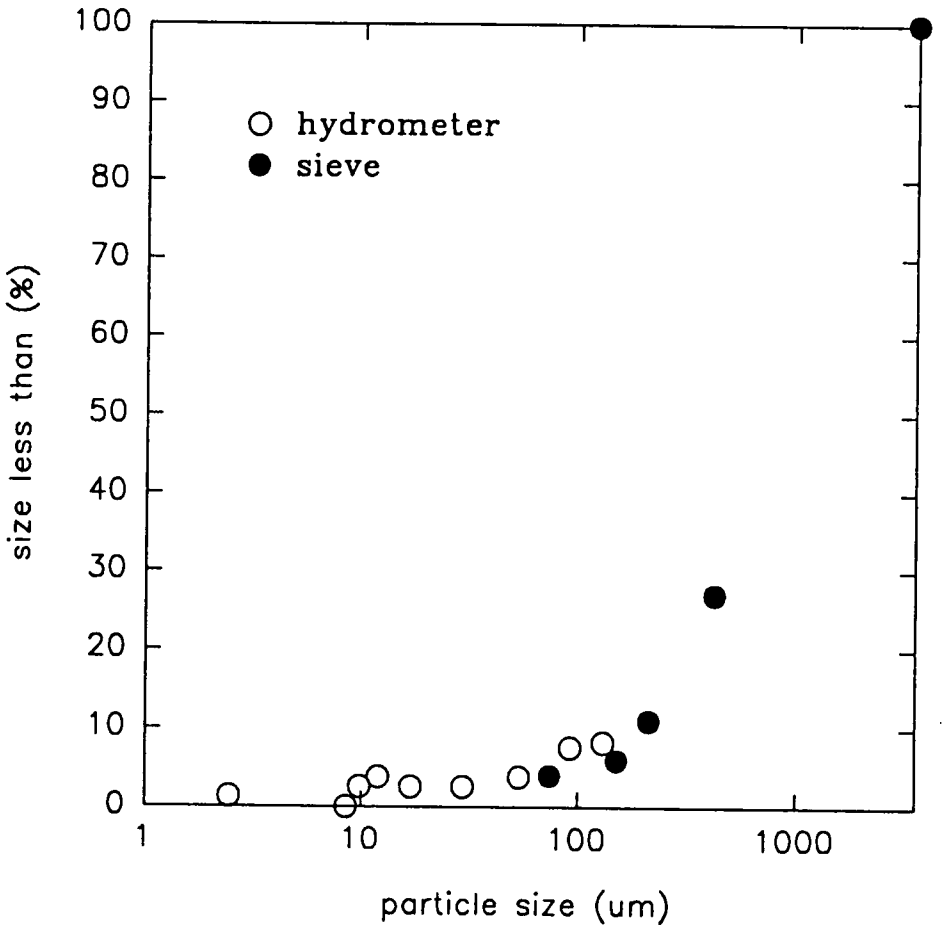

Figure 4.2 GRI Soil Particle Size Distribution

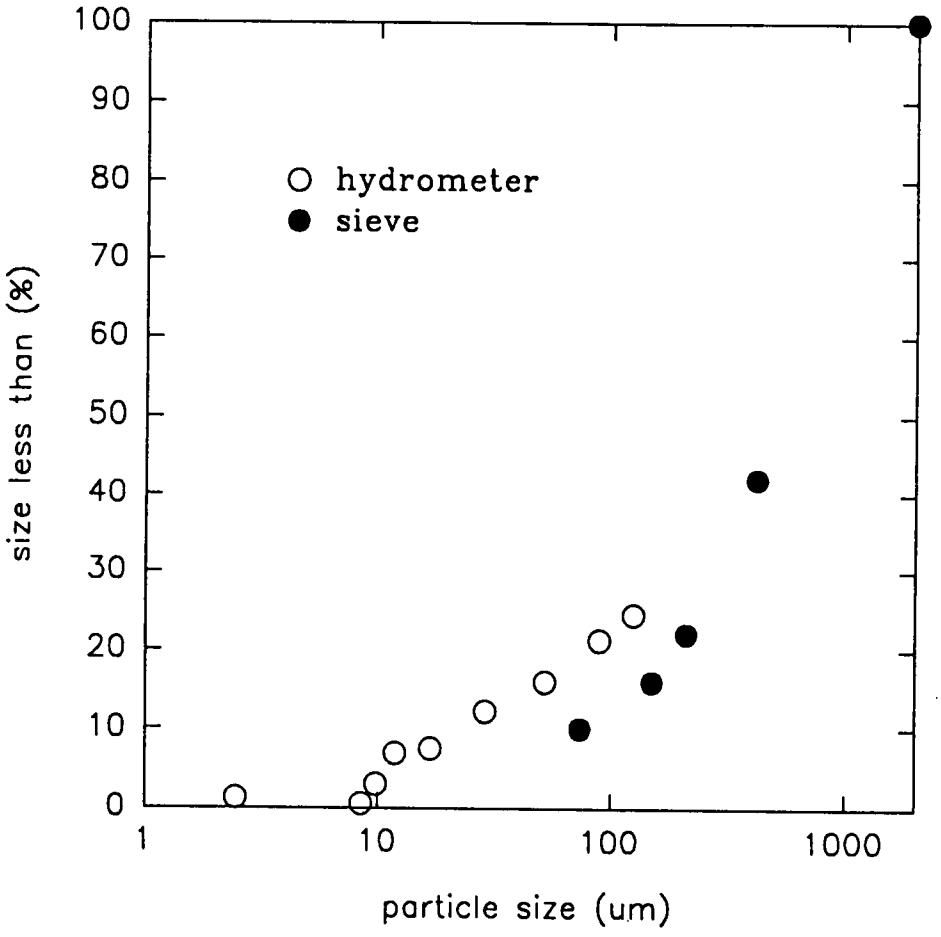

Figure 4.3 TN Soil Particle Size Distribution

Table 4.1 Particle density, carbon content, and total aerobic heterotrophs of soils.

Soil Name	Particle Density ρ_s (g/mL)	Carbon Content (%)	Microbial Population TAH (CFU/g)
ART	2.45	1.97	N/A
GRI	1.72	68	5.02×10^3
TN	1.53	42	5.80×10^6

density is greatest for ART soil and smaller for GRI and TN soils. This can be attributed to the high organic carbon content of the GRI and TN soils. Organic matter is less dense than soil minerals and the coal-tar coating may block some pore entrances. Carbon content is the mass fraction of carbon contained in a known mass of soil and is defined as (% carbon = mass carbon / total soil mass * 100 %). The GRI and TN soils have very high carbon contents associated with the heavy contamination on each soil. In the case of the GRI soil, over half the sample weight is carbon. Total aerobic heterotrophs (TAH) refers to the number of colony forming units (CFU) per unit mass of soil; the TN soil was found to have a TAH count almost 3 orders of magnitude greater than GRI soil.

The TN and GRI soils were also analyzed to determine anthropogenic contaminant loadings. Triplicate soxhlet extractions were performed on each soil to estimate the loading for fluorene, phenanthrene, and anthracene. This extraction procedure was not performed on the ART soil because it was not previously contaminated. Results from each soxhlet extraction and estimates of the mean and standard error are reported in Table 4.2. The table shows that the GRI soil is much more heavily contaminated than the TN soil for the three PAHs of interest.

Table 4.2 Soxhlet Extraction Data for TN and GRI Soils

Soil Name	Soxhlet Extraction A (ug/g)	Soxhlet Extraction B (ug/g)	Soxhlet Extraction C (ug/g)	Mean (ug/g)	Standard Error (%)
TN	Fl=22 Ph=39 An=8	Fl=22 Ph=32 An=6	Fl=25 Ph=39 An=8	Fl=23 Ph=37 An=7	Fl=7 Ph=12 An=13
GRI	Fl=130 Ph=225 An=58	Fl=127 Ph=225 An=61	Fl=111 Ph=251 An=63	Fl=123 Ph=234 An=61	Fl=8 Ph=6 An=4

4.2 Gas Purge Studies

The results and interpretations of the gas purge experiments are presented in this section. Initially, the solution purge experiments are discussed. Then, the experiments conducted with the artificially contaminated soil are presented, followed by the data obtained from experiments performed with anthropogenically contaminated soils.

All gas-purge data are reported as % recoverable PAH, defined as:

$$\%\ recoverable\ PAH = \frac{cummulative\ mass\ desorbed\ at\ time=t}{total\ recoverable\ PAH}$$

The total recoverable PAH is defined as the total PAH recovered from all the traps plus the PAH extracted from the soil-water suspension after purging. The % recovery for a given experiment is calculated as a check on the over all mass balance:

$$\%recovery = \frac{total\ recoverable\ PAH}{initial\ PAH}$$

4.2.1 Solution Purge Experiments

Two experiments in which PAHs were purged from aqueous solution were conducted to characterize the aqueous-to-air mass transfer and recovery efficiencies. The experiments were performed by preparing an aqueous solution with known concentrations of three PAHs (fluorene, phenanthrene, and anthracene) and stripping them from solution using the gas purge apparatus. The stripped PAHs were trapped in Tenax resin traps, extracted, and quantitated with HPLC.

These experiments, designated as SP200 and SP400, were designed to give compound-specific information characterizing the mass transfer to the gas phase. The rate of PAH removal and mass recovery efficiencies, including errors relating to HPLC analysis, pipetting, dilution, and Tenax trap extraction efficiency, can be determined from these experiments.

Experiments SP200 and SP400 were performed under identical conditions, except initial PAH concentrations in SP200 ranged from 60 - 80 % of saturation while those of SP400 were approximately 50 % of saturation. Experimental conditions are summarized in Table 3.1.

Removal of fluorene, phenanthrene, and anthracene in

experiments SP200 and SP400 are shown in Figures 4.4 and 4.5, respectively. In both experiments, approximately 100 % of the recoverable PAH is removed from solution after 15 hr of purging. Removal of the first 95 % of the PAHs occurs in approximately 8 to 10 hours, while removal of the remaining 5 % requires another 15 hours. Fluorene is removed from solution fastest; phenanthrene and anthracene are removed slower. Percent recovery, defined as:

$$\%recovery = \frac{totalrecoverablePAH}{addedPAH} \times 100\%$$

They are shown for each PAH in Table 4.3; they range from 81 - 111 %. Variation from 100 % recovery appears to be random in nature and can probably be attributed to various types of experimental error. The most probable sources of error are: (1) weighment of PAHs for stock solution, (2) micro-syringe spiking of aqueous solution, (3) loss of PAH on apparatus surfaces, (4) loss through Tenax traps, (5) extraction efficiency of PAHs from Tenax traps, and (6) HPLC analysis. In general, experiments involving "trace" quantities of organic compounds are subject to experimental artifact.

Mackay et al. (1979) state that stripping PAHs from the aqueos phase should follow first order kinetics (ln of the solute remaining vs. time is linear), provided that the following assumptions are valid: (1) isothermal system, (2)

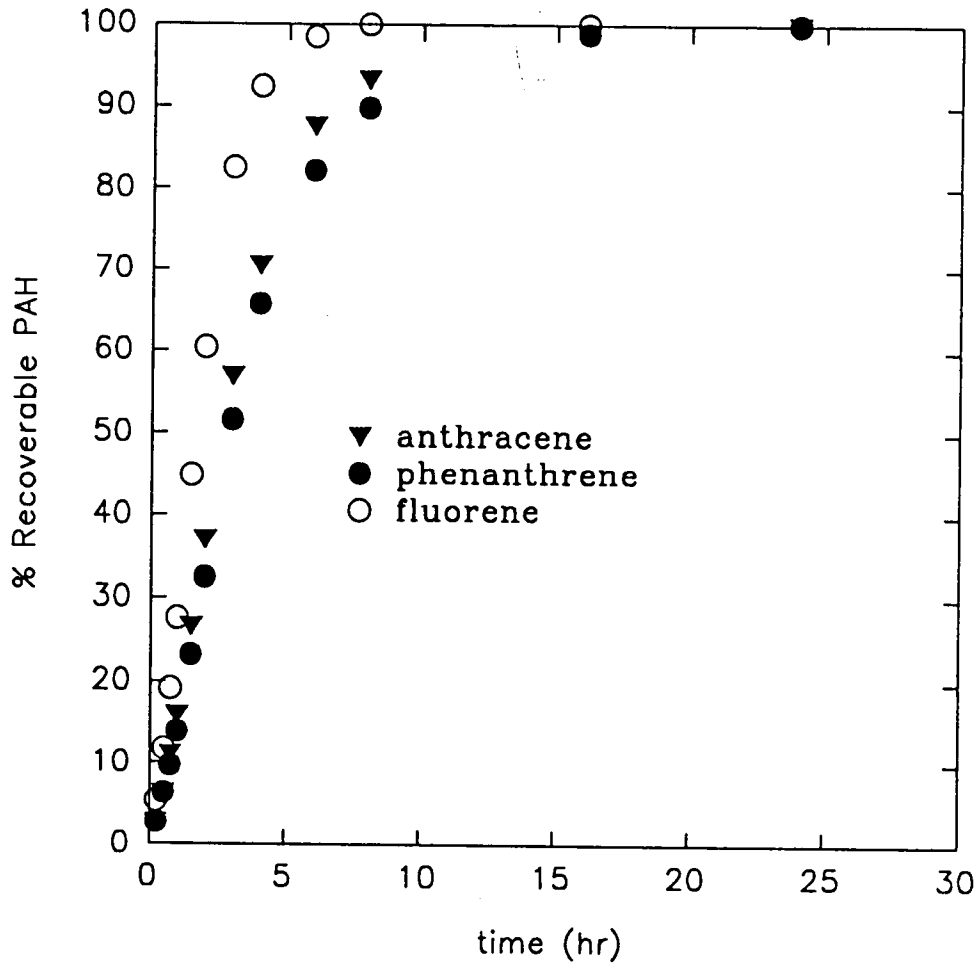

Figure 4.4 PAH Removals From Solution During Gas Purge as a Function of Time for Experiment SP200

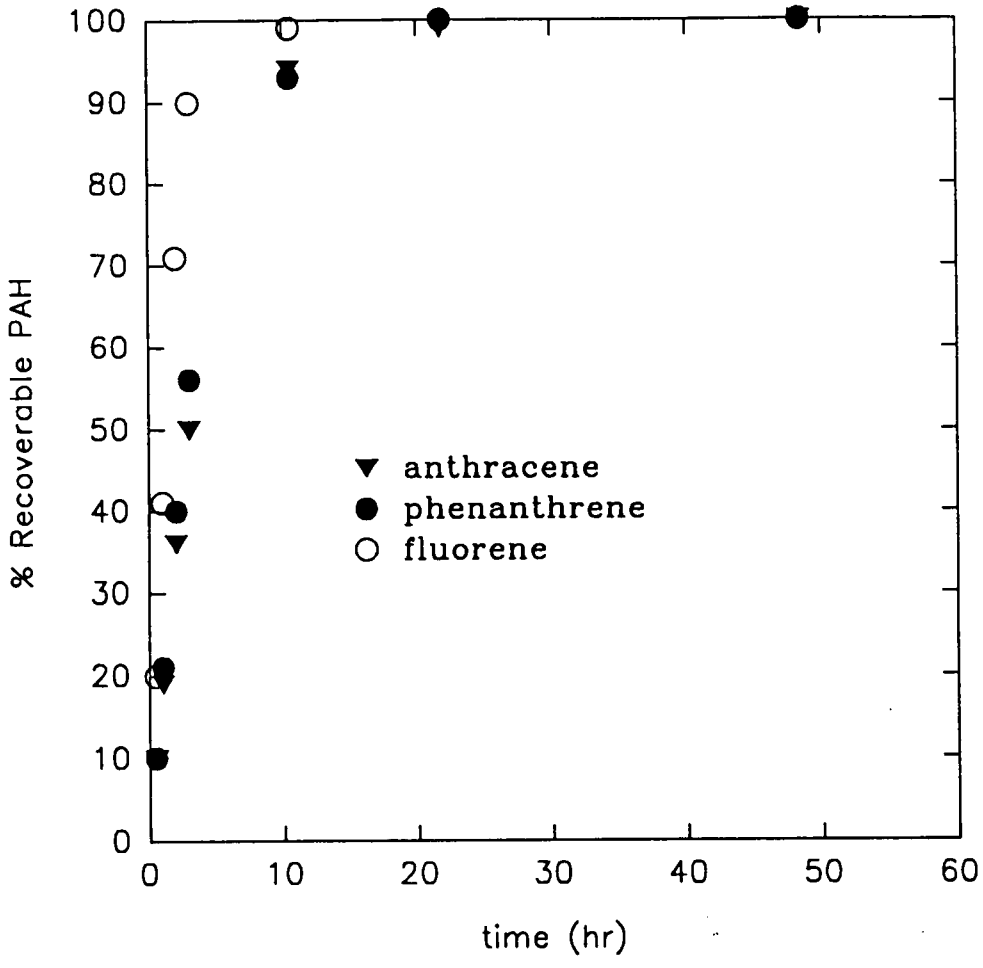

Figure 4.5 PAH Removals From Solution During Gas Purge as a Function of Time for Experiment SP400

Table 4.3 Summary of Experimental Recoveries

Experiment Name	Recoveries (%)
SP200	fl - 92 ph - 85 an - 100
SP400	fl - 81 ph - 111 an - 96
ART2d	ph - 104
ART20d	ph - 106
ART10m	ph - 93
ARTGRI	ph - 79
GRI	fl - 117 ph - 122 an - 50
TN	fl - 38 ph - 67 an - 38
TNCLDN2	fl - 120 ph - 72 an - 66

well mixed system, (3) ideal vapor behavior, (4) concentration of solute obeys Henry's law, (5) constant liquid volume, (6) total pressure is large compared to the solute vapor pressure, and (7) solute in the exit vapor is equilibrated with the solute in the liquid phase. Figures 4.6 and 4.7 confirm that the removal of fluorene, phenanthrene, and anthracene follow first order kinetics. The mass fraction remaining is calculated using the cummulative mass purged as the initial mass. Linear regression is used to fit lines through data points for each PAH, and a rate constant is calculated from the slope. Equation 4.1 describes the removal of a PAH from solution.

$$\frac{dC_{aq}}{dt} = -k_g C_{aq} \qquad 4.1$$

where:

C_{aq} = solute aqueous concentration

t = time

k_g = mass transfer constant from aqueous to gas phase

The rate constant, k_g, quantitatively describes the removal of a specific PAH from the aqueous phase for a given set of conditions. The equation states that the change in aqueous concentration of a solute with time equals aqueous concentration multiplied by a specific rate constant. k_g

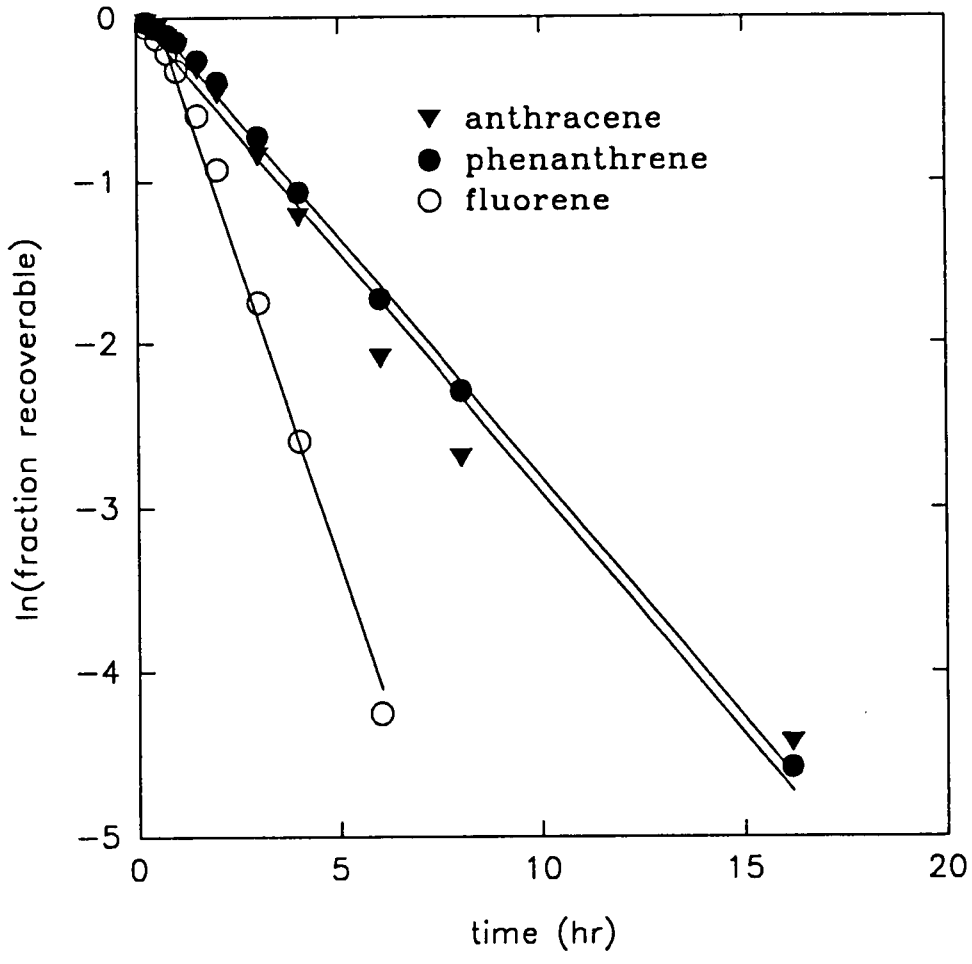

Figure 4.6 Determination of Solution-To-Air Mass Transfer Rate Constants for Experiment SP200

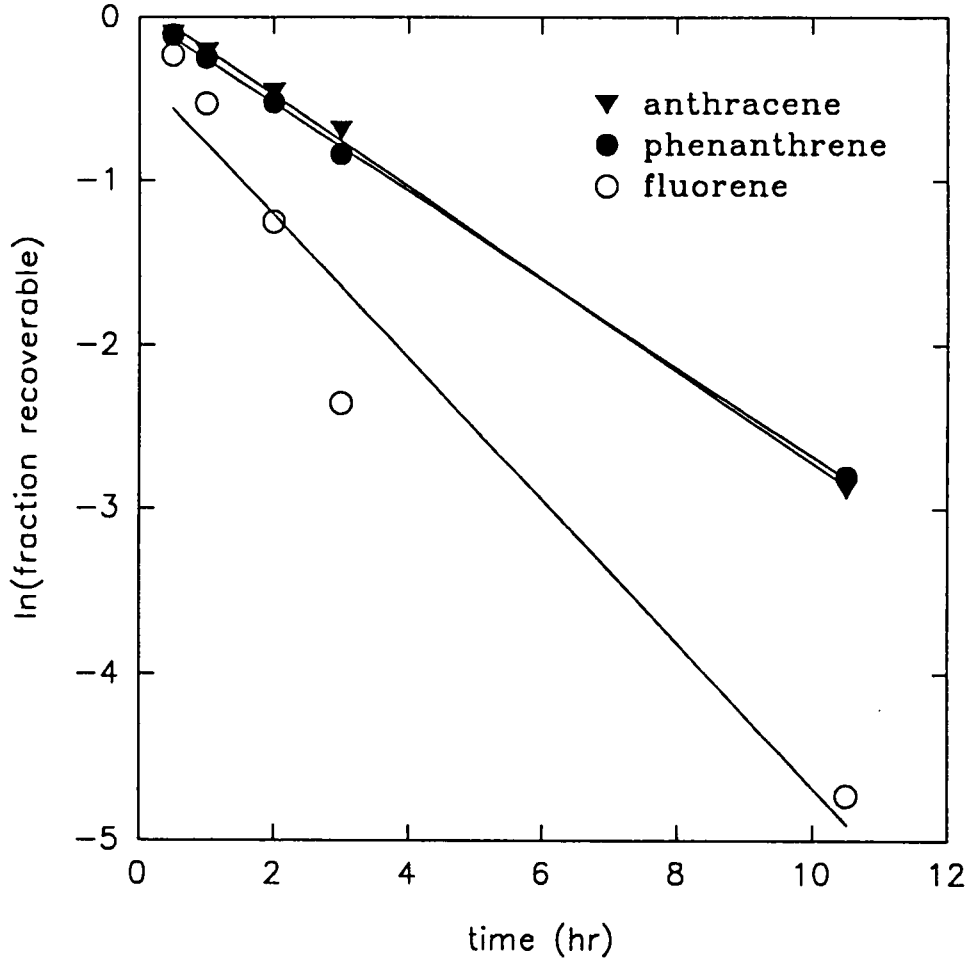

Figure 4.7 Determination of Solution-To-Air Mass Transfer Rate Constants for Experiment SP400

can be further defined as follows (Mckay et al., 1979):

$$k_g = \frac{H_{app} G}{VRT} \qquad 4.2$$

where:

H_{app} = apparent Henry's constant

= $H(1-\exp(-K_{OL}ART/GH))$

H = Henry's constant

K_{OL} = overall aqueous-gas mass transfer coefficient

A = interfacial area

G = gas flow rate

V = aqueous volume

R = gas constant

T = temperature

In both solution purge experiments, regression lines are fitted to data points for each compound and first-order rate constants are calculated from the slopes. An apparent Henry's constant is then calculated from each rate constant using Equation 4.2. Table 4.4 lists effective rate constants, apparant Henry's constants, and literature values for Henry's constants. k_g values for phenanthrene and anthracene show good agreement when comparing SP200 and SP400 data, but the rate of removal for fluorene in SP200 is much larger than in SP400. However, for each PAH, the rate constant is larger in SP200 than in SP400. The apparent

Table 4.4 Rate and Henry's Constants Summary

Constant	SP200	SP400
k_q (hr^{-1})	fl = 0.743 ph = 0.293 an = 0.293	fl = 0.434 ph = 0.269 fl = 0.281
H_{app} (L-atm/mol)	fl = 7.47×10^{-2} ph = 2.94×10^{-2} an = 2.95×10^{-2}	fl = 4.36×10^{-2} ph = 2.70×10^{-2} an = 2.82×10^{-2}
H_L[1] (L-atm/mol)	fl = 8.39×10^{-2} ph = 3.95×10^{-2} an = 5.92×10^{-2}	
H_L[2] ($Pa-m^3/mol$)	fl_{max} = 33.4 fl_{min} = 5.06 ph_{max} = 22.90 ph_{min} = 0.691 an_{max} = 73.0 an_{min} = 1.80	

[1] Recomended literature values for Henry's constants (Mckay and Shiu, 1981).

[2] Literature values vary greatly as given by Mckay et al. (1992). Maximum and minimum values are reported to show variation.

Henry's law constants follow these same trends. The most probable explanation for non-agreement in the two experiments is given by noting the possibility of experimental artifact. Despite the variability, the Henry's constants calculated from the rate constants show reasonable agreement with Henry's constants taken from literature, suggesting that the gas exiting the apparatus is in equilibrium with the aqueous phase.

4.2.2 Artificially Contaminated Soils

In these experiments, soils were contaminated artificially with ^{14}C-labeled phenanthrene. The soil was contaminated using a phenanthrene stock solution; a fraction of the total phenanthrene was radiolabeled. This solution was added to glass centrifuge tubes containing a known mass of soil. The tubes were sealed and stored until the desired contamination age was reached. Three experiments were conducted with the ART soil (experimental details summarized in Table 3.2). Purge experiments were conducted with this soil at contamination ages of 2 days, 20 days, and 10 months (ART2d, ART10d, and ART10m). The fourth experiment was conducted with the previously contaminated GRI soil. In this experiment, the soil was augmented with labeled phenanthrene and purged following a 5-day contamination age period (ARTGRI). When a desired contamination age was

reached for a soil, the aqueous supernatant was analyzed to determine the mass of phenanthrene in solution. Sorbed mass was determined by difference. From this information apparent K_p's were calculated for each soil as follows: (1) ART2d - K_p = 0.220 L/g, with 94.6 % mass sorbed and 5.4 % mass in solution, (2) ART20d - K_p = 0.268 L/g, with 95.6 % mass sorbed and 4.4 % mass in solution, (3) ART10m - K_p = 0.231 L/g, with 94.9 % mass sorbed and 5.1 % mass in solution, (4) ARTGRI K_p = 46.5 L/g, with 99.5 % mass sorbed and 0.5 % mass in solution.

Figure 4.8 shows the percentage of recoverable phenanthrene purged as a function of time. For ART2d and ART20d, essentially all of the recoverable phenanthrene was desorbed following approximately two weeks of desorption. Only 79 % of recoverable phenanthrene was desorbed from ART10m soil in approximately the same desorption time period. Recoveries, reported in Table 4.3, are determined by dividing the cummulative reocoverd mass by the initial measured mass as follows:

$$\%recovery = \frac{total\ recoverable\ PAH}{initial,\ PAH\ loading\ on\ soil} \times 100\%$$

Quantitative recovery of phenanthrene within +/- 10 % is

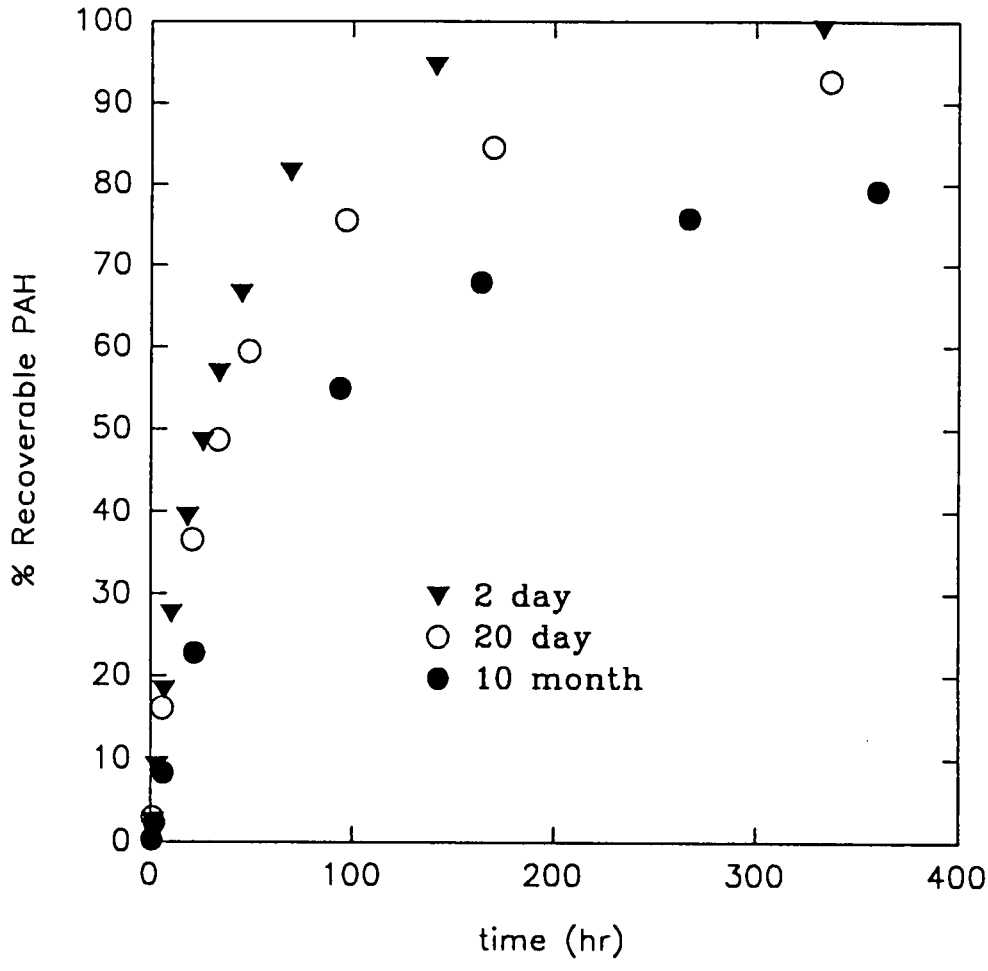

Figure 4.8 Phenanthrene Removal as a Function of Time in the ART Experiments

achieved for these three experiments.

It can be seen that desorption rate is inversely proportional to contamination age (e.g. desorption rate for ART2d is faster than for ART10m). This characteristic is also reported by Pavlostathis and Mathavan (1992). This characteristic is readily observable when comparing ART2d and ART10m. However, the desorption rate difference between ART2d and ART20d is not as apparent. The rate of ART20d is slightly less than that for ART2d and may not be significantly distinguishable due to experimental variance. Some recoveries are greater than 100 %, an artifact that can most likely be attributed to analytical variance between samples. Variance between quenching calibration curves for aqueous samples and organic samples in LSC analysis may also contribute.

Desorption of phenanthrene from soil shows a biphasic pattern. Karickhoff and Morris (1985), as well as numerous others, substantiate this finding. Initially, there is a fraction which is quickly desorbed. The remianing phenanthrene requires much longer to desorb. It appears that the fraction which is more easily desorbed is inversely proportional to contamination age. This characteristic can be linked to diffusion of phenanthrene into the soil particles as a function of increasing contamination age. As

diffusion proceeds, the time and difficulty to desorb phenanthrene become greater. Ideal kinetic reversibility is not apparent when comparing the amount of time required for adsorption and desorption. For example, in the ART2d experiment it only requires 2 days to achieve approximately 95 % adsorption of the phenanthrene present in the original contaminant solution. In the desorption experiment, only 67 % of the mass is removed during the first two days. The data shows that the effect of nonequilibrium increases with contamination age. There is some lag period between phenanthrene desorption and transfer to the gas phase; however, this is very small compared to the desorption time periods for these experiments.

The model described by Karickhoff and Morris (1985) is used to evaluate the desorption rate of phenanthrene from the ART soil experiments. The model, described in section 2.2.2, represents desorption from spherical particles as an infinite-depth planar source. The system can be represented by this idealized geometry during the initial portion of the desorption experiments. In this case the fractional desorption is proportional to the square root of time:

$$f_s(t) = k_s t^{1/2} \qquad 4.3$$

where:

$f_s(t)$ = fraction of adsorbate released

k_s = diffusive constant

t = time

The diffusive constant is related to the soil structure, sorbate characteristics and the effective diffusion coefficient for a particular system. Figure 4.9 shows the fraction of total phenanthrene desorbed as a function of the square-root of time for each ART soil experiment. A linear regression is fitted to the data for calculation of diffusive constants. However, only data points for which the idealized-geometry is valid are included in the regression analysis. For the ART2d experiment, the last two data points are omitted, and for the ART20d and ART10m experiments the last three data points are omitted. The omitted data points occur during the end of the experiment when the idealized-geometry approximation is no longer valid. Non-linearity at the end of desorption is caused by exhaustion of the compound source. At this point, the system does not simulate an infinite depth/planar source model. But, as Figure 4.9 shows, the majority of desorption follows a linear trend. This linearity is extended farther as contamination age decreases due to position of adsorbate within soil particles and the relative ease of compound desorption. The slope of a line through a particular set of data corresponds to the diffusive constant, k_s, with units of $hr^{-1/2}$. Included in Figure 4.9 is the diffusive constant for each ART soil experiment. The constants range from 0.11

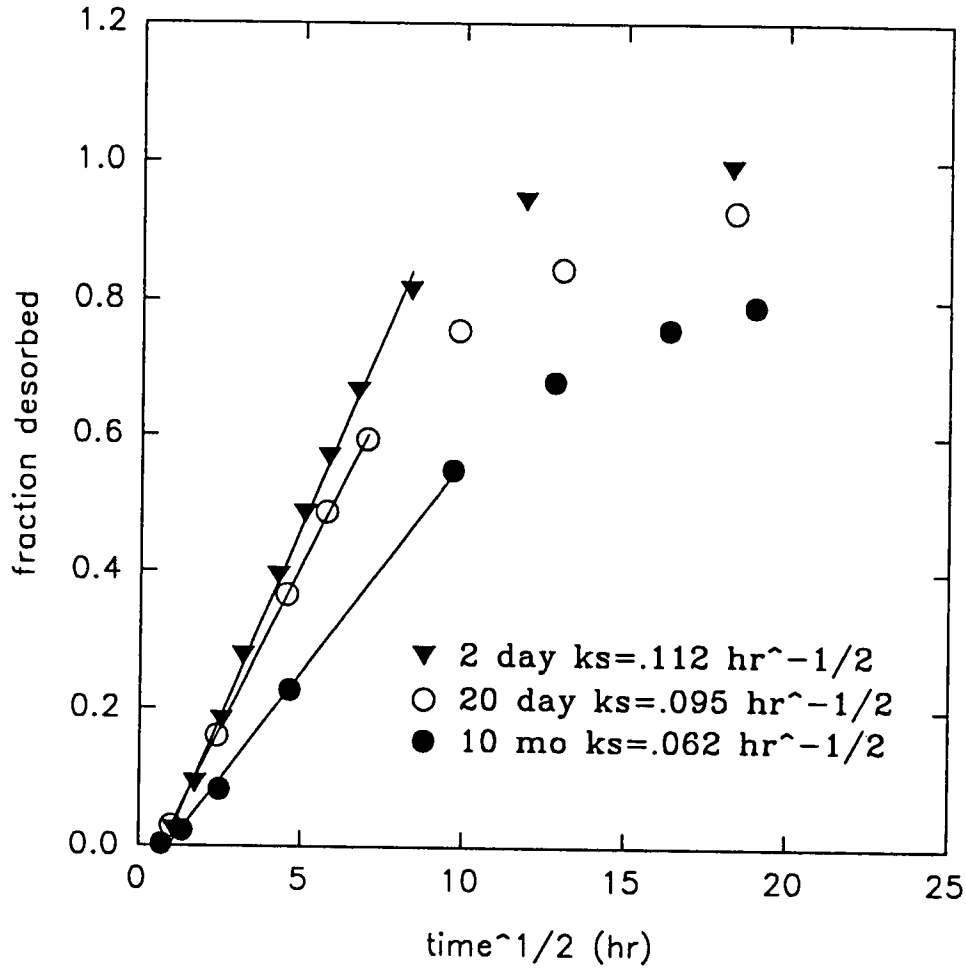

Figure 4.9 PAH Fraction Desorbed as a Function of the Square-Root of Time in the ART Experiments

$hr^{-1/2}$ for ART2d to 0.06 $hr^{-1/2}$ for ART10m. The trend shows that the diffusive constant decreases with increasing contamination age. A similar trend was recently reported by Harmon and Roberts (1994). The rate constants given above are only applicable over the desorption range shown in the figure.

Figures 4.10 and 4.11 show the same interpretations for the ARTGRI data. The most obvious trend shows the dramatic decrease in desorbed phenanthrene over a two week desorption period. Approximately 6 % of the artificially spiked mass desorbed in this period. The very small curvature at the beginning of the desorption period, which is indicative of the readily desorbed fraction, quickly levels off and becomes asymptotic. This behavior can be explained when considering the previous state of the GRI soil. It is very heavily contaminated with coal tar and has an extremely high affinity for newly added contaminants. The contaminant will probably exhibit this same type of slow "bleeding" desorption trend irrespective of contamination age. This is primarily due to the huge affinity the adsorbent has for the adsorbate. Figure 4.11 shows the total mass fraction desorbed versus the square-root of time for the ARTGRI data. All data points are used for determination of k_s due to excellent linearity throughout the desorption period. k_s for this data is much smaller than those given for ART2d,

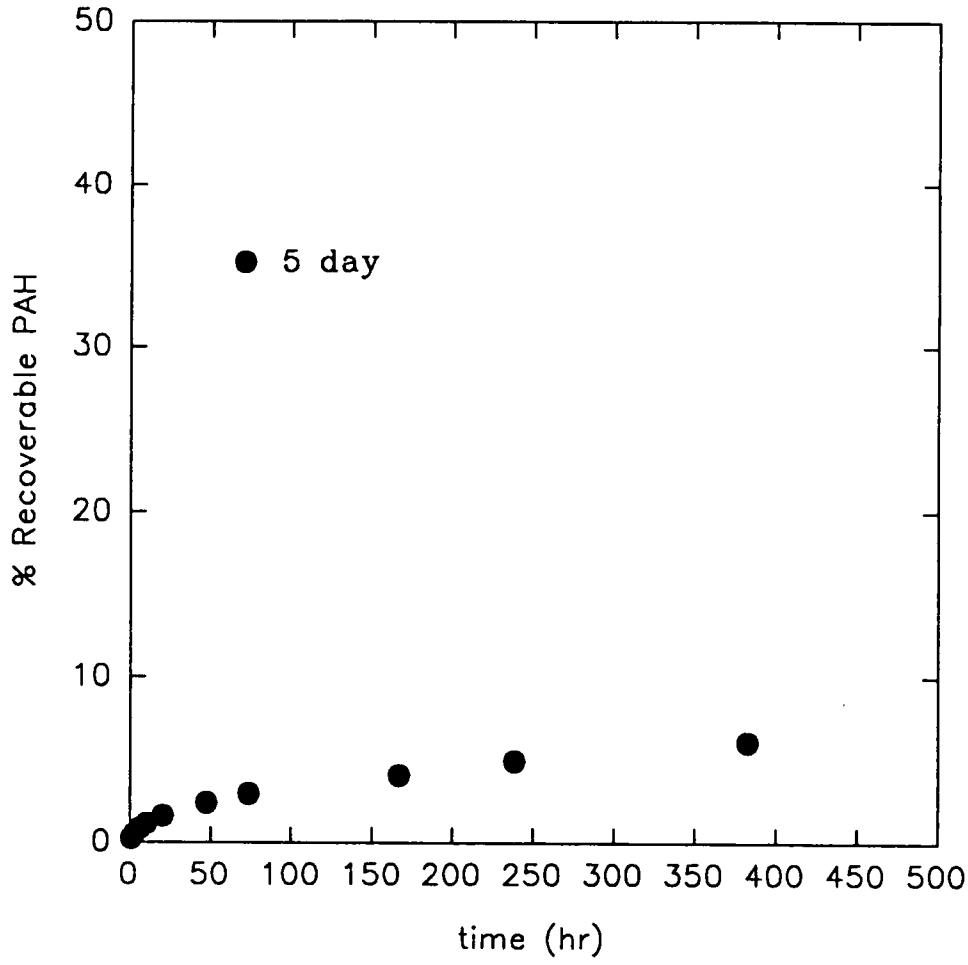

Figure 4.10 Phenanthrene Removal as a Function of Time in the ARTGRI Experiment

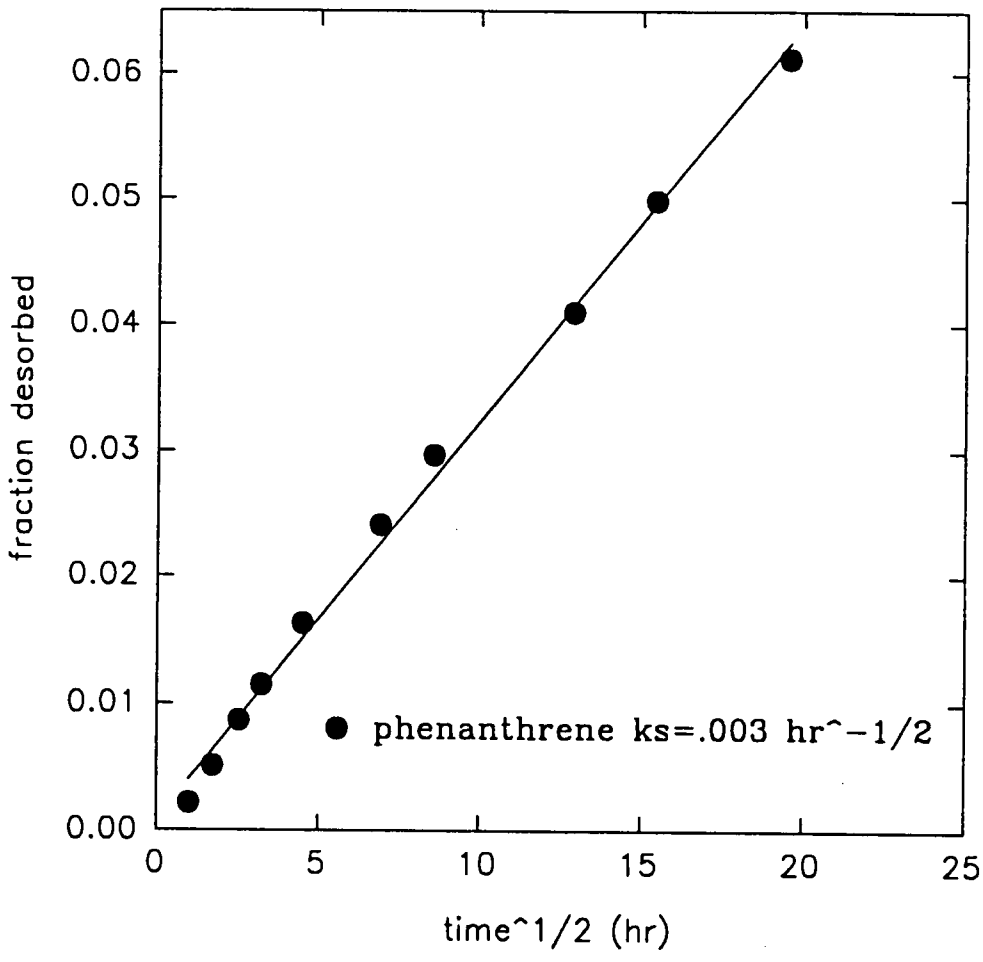

Figure 4.11 Phenanthrene Removal as a Function of the Square-Root of Time in the ARTGRI Experiment

ART20d, and ART10m. This rate constant characterizes the desorption very well throughout the entire experimental period.

4.2.3 Anthropogenically Contaminated Soils

Three separate experiments were conducted with anthropogenically contaminated soils. The TN soil was used in two experiments (TN and TNCLDN2) and the GRI soil was used in the other (GRI). Experimental conditions, soil history, and soil characterizations are summarized in Table 3.3, Section 3.1.1, and Section 4.1, respectively. The soils were purged for periods ranging from 21 to 31 days. The major difference between the two TN experiments was that one was performed at 4 °C with nitrogen as purge gas ($TNCLDN_2$), while the other experiment was conducted at room temperature with air (TN). Overall, the experiments were conducted as follows: (1) a known mass of anthropogenically contaminated soil was added to the stripping flask containing a 650 mg/L sodium azide solution, (2) a gas source was selected and used at the desired flow rate, (3) traps were taken throughout the experiments, extracted, and analyzed by HPLC, and (4) the soil was consolidated after purge for recovery of remaining contaminants. Data analysis will be presented first for the GRI experiment and then for the TN and $TNCLDN_2$ experiments.

Figure 4.12 shows the percentage of recoverable PAH desorbed in the GRI experiment as a function of time for PAH compounds fluorene, phenanthrene, and anthracene. Mass recoveries, given in Table 4.3, were calculated from:

$$\%recovery = \frac{total\ recoverable\ PAH}{PAH\ initial\ soxhlet} \times 100\%$$

Percent recovery is based on the ratio of cummulative recovered mass to mean soxhlet mass for a particular compound. For example, only 50 % of the fluorene soxhlet mean could be accounted for after adding the cummulative purged mass to the remaining mass extracted from the soil following the purge period. In the case of phenanthrene, 22 % more mass was recovered than expected from the soxhlet mean.

The expected errors in this experiment were calculated by propogation analysis in Appendix B. The standard error for % recovery was calculated to be 15 % for fluorene and 19 % for phenanthrene and anthracene. A comparison of the standard errors to the % recoveries (17 %, 122 %, and 50 %, respecitvely) suggests that some additional losses of anthracene may be occuring. Recovery of fluorene and phenanthrene are within the expected error.

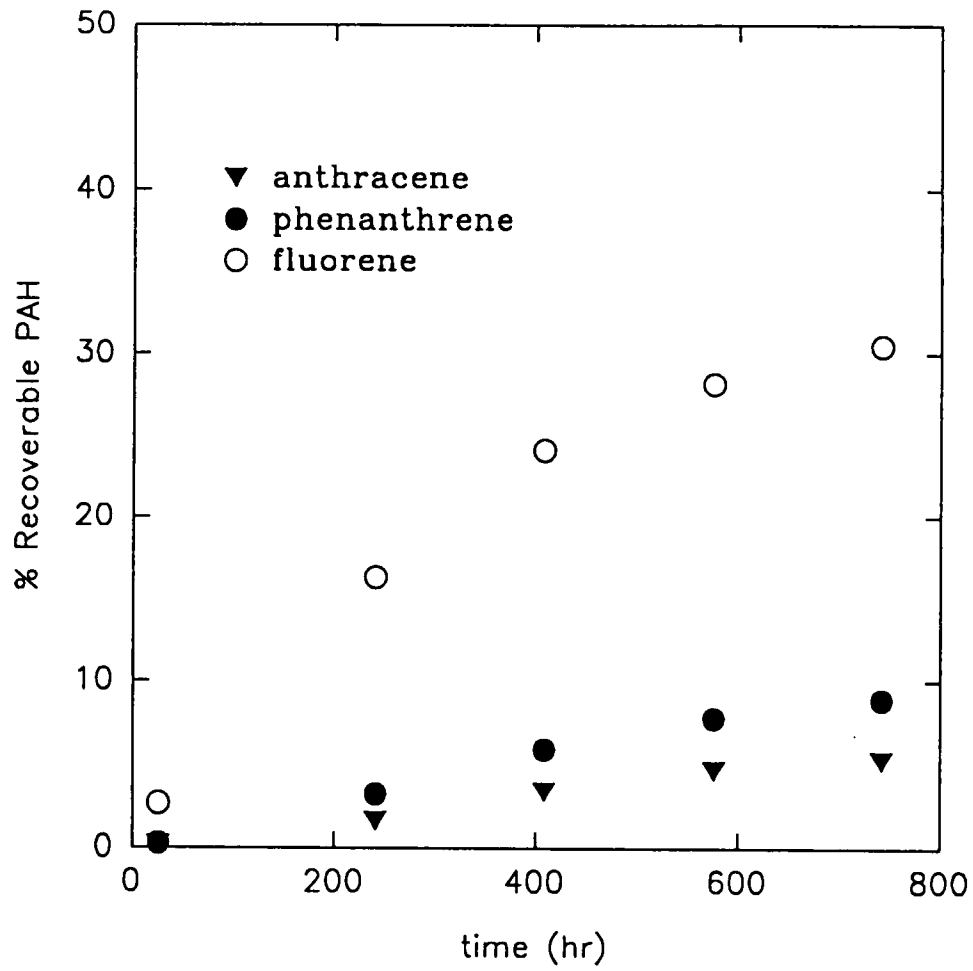

Figure 4.12 PAH Removals as a Function of Time in the GRI Experiment

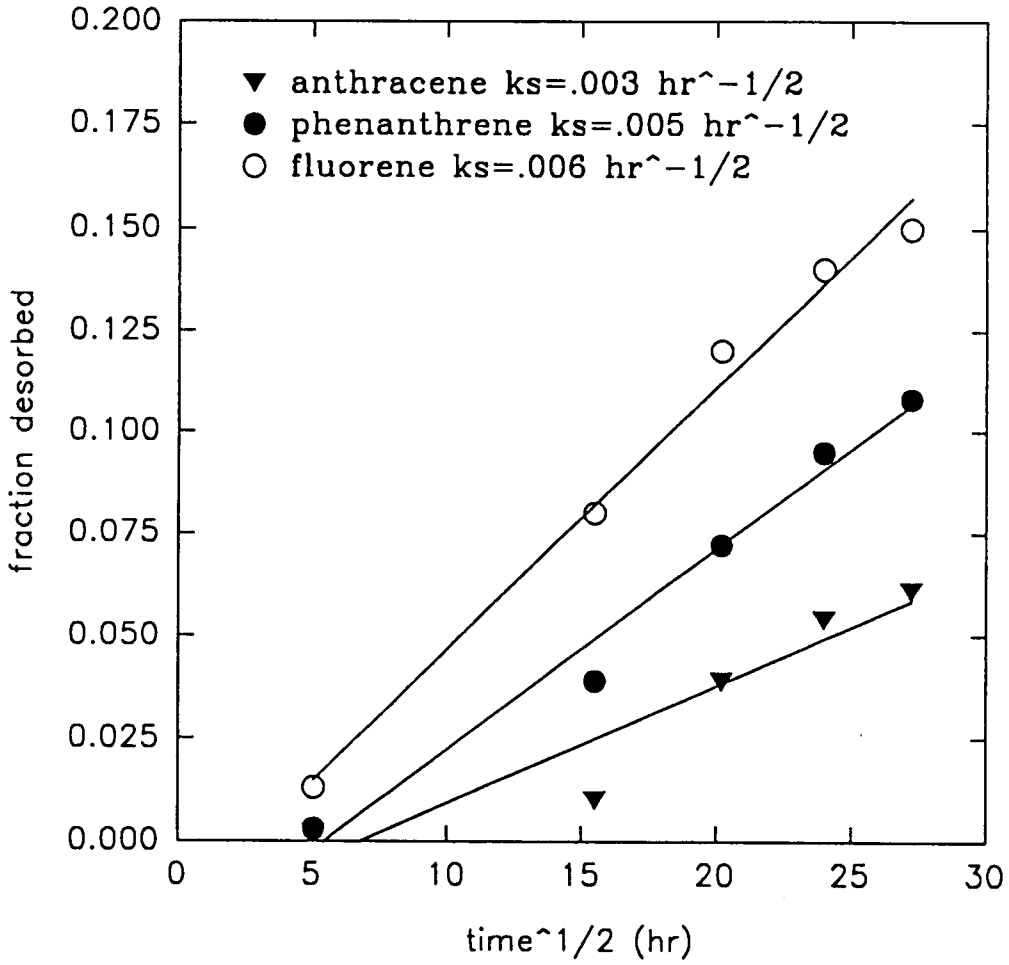

Figure 4.13 PAH Removal as a Function of the Square-Root of Time in the GRI Experiment

Percent desorption is based on the ratio of accumulated purged mass to total recovered mass. After 742 hr of purging, 30 % fluorene, 9 % phenanthrene, and 5 % anthracene were desorbed from the GRI soil. The desorption curves do not exhibit an obvious biphasic shape as compared with the ART experiments. This is a result of the very long contamination age of the GRI soil and the very high affinity the soil has for PAH compounds. Fluorene removal is somewhat curvilinear, while phenanthrene and anthracene show near linearity. Table 4.5 shows literature values for solubility (Schwarzenbach et al., 1993). The table includes the aqueous solubility of both the solid and subcooled-liquid PAHs. The desorption rate is expected to be correlated with the subcooled-liquid solubilities, C_A^L. Fluorene, characterized by the greatest value of C_A^L, desorbs most rapidly and the desorption rates of phenanthrene and anthracene, compounds characterized by similar values of C_A^L, are equal within the error of the experiment.

Desorption data from the ARTGRI and GRI experiments are combined for phenanthrene and presented in Figure 4.14. Anthropogenic and labeled phenanthrene desorb at essentially the same rate; however, it would be expected that the labeled phenanthrene would desorb faster than the anthropogenic phenanthrene due to its shorter contamination

Table 4.5 Solubility Data for PAHs of Interest

Parameter	Fluorene	Phenanthrene	Anthracene
log C_A^S	-4.96	-5.20	-6.46
log C_A^L	-4.08	-4.46	-4.48

C_A^S Aqueous solubility for pure solid.
C_A^L Aqueous solubility for pure subcooled liquid.

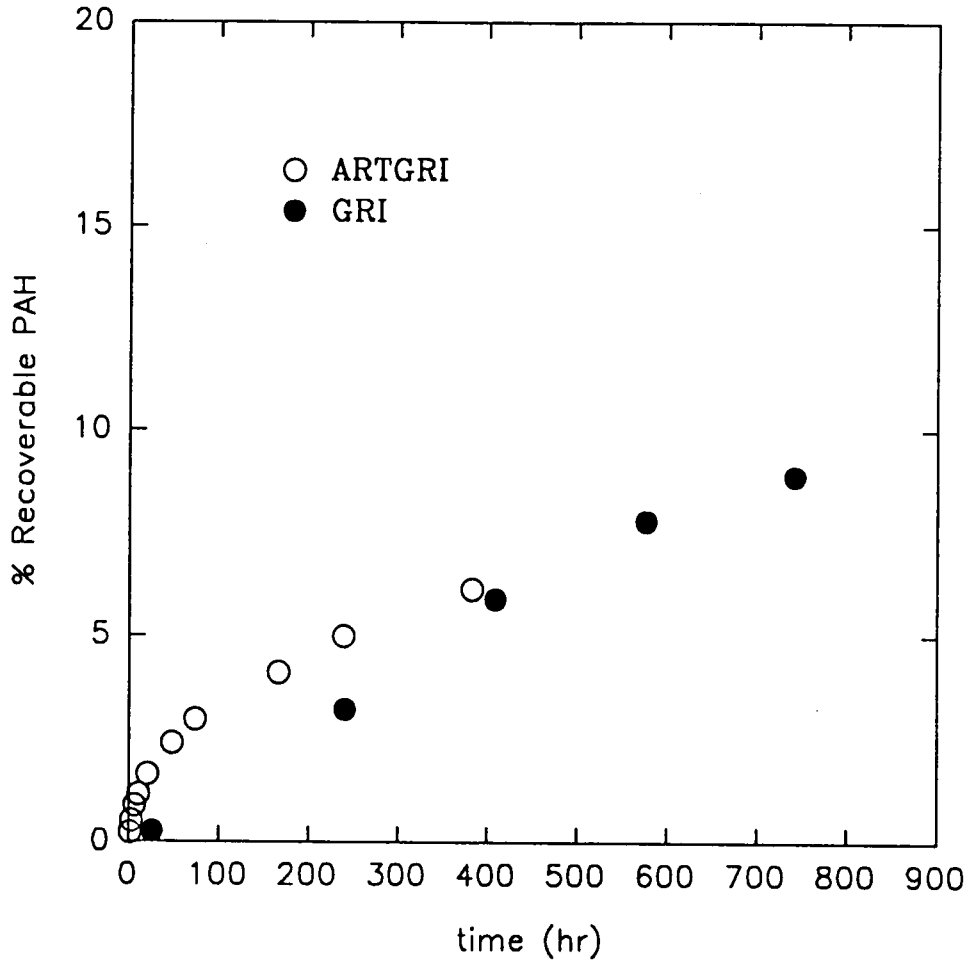

Figure 4.14 Removal of Phenanthrene as a Function of Time in the ARTGRI and GRI Experiments

age. One may speculate that the phenanthrene is not uniformly distributed through the particle. The other ART experiments show much greater desorption rates for contamination ages similar to the ARTGRI experiment. This suggests that soil properties may play a more important role than contamination age in determining desorption rates.

Figure 4.15 shows the results of the TN soil experiment, with initial contaminant loadings given in Table 4.2. In these plots, the biphasic pattern of desorption is slightly more apparent. This may be a result of lower contaminant affinity, due to the smaller contaminant loading per unit mass of soil (relative to GRI soil). After 762 of continuous purging, 37 % of anthracene, 30 % of fluorene, and 11 % of phenanthrene are removed. In this experiment, the desorption trends do not follow sub-cooled liquid solubilities. k_s values are listed in Figure 4.16, with anthracene showing the fastest desorption rate and phenanthrene showing the slowest.

The error propagation analysis (Appendix B) indicates that standard errors of 17 % to 19 % should be expected in the mass recoveries. Mass recoveries reported in Table 4.3 were unacceptably low for this experiment, given the expected standard errors. Biodegradation was suspected as the cause, the presence of biocide notwithstanding. As

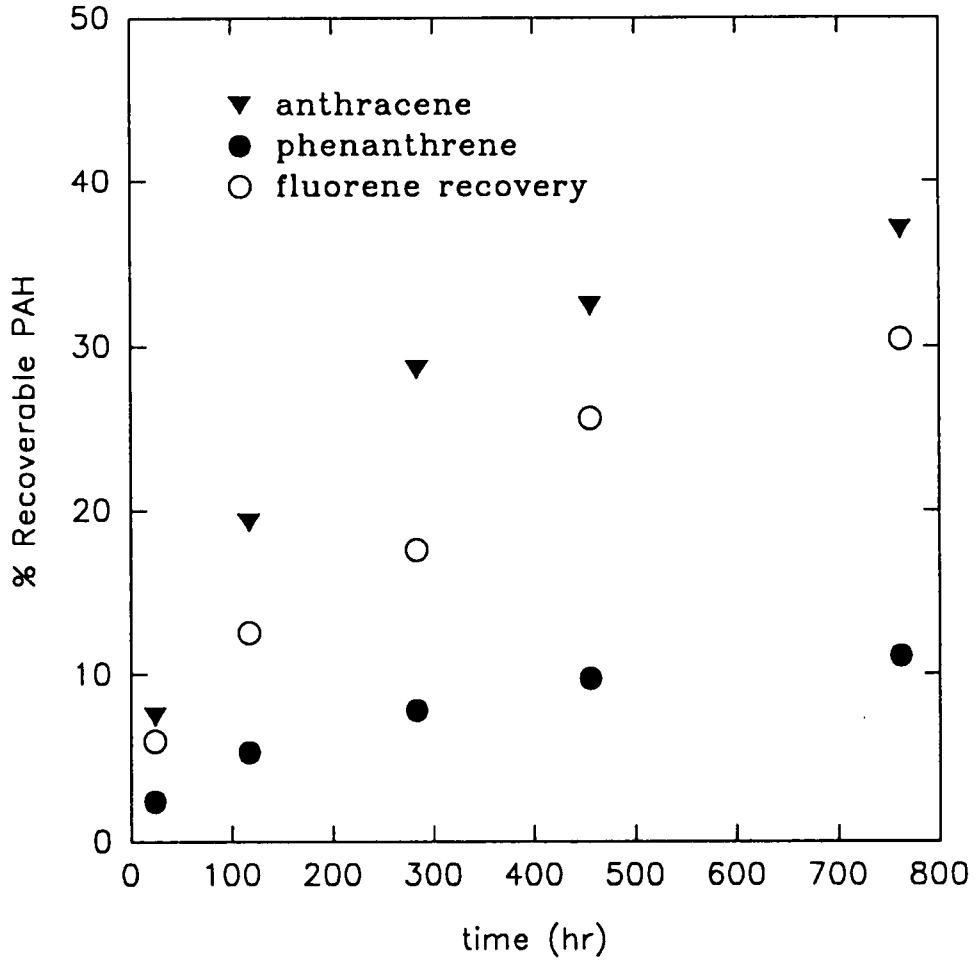

Figure 4.15 PAH Removals as a Function of Time in the TN Experiment

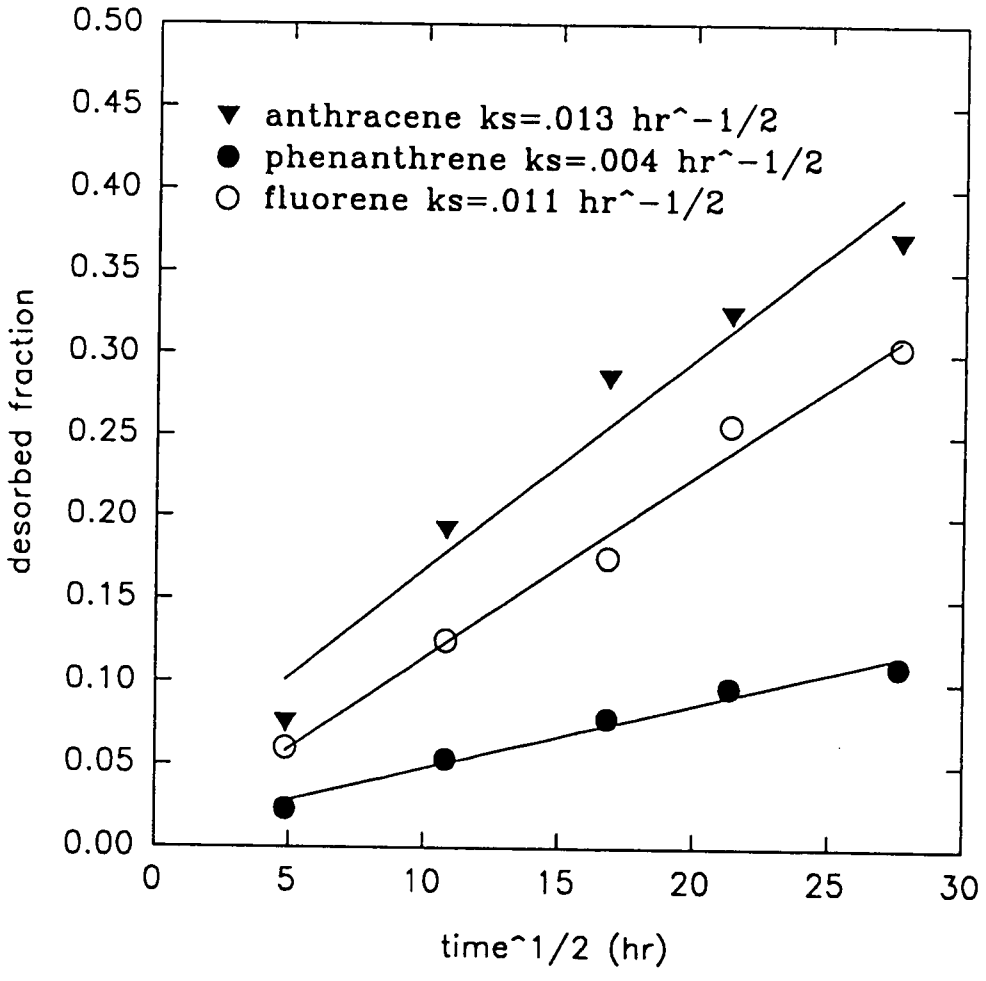

Figure 4.16 PAH Removals as a Function of the Square-Root of Time in the TN Experiment

noted in Table 4.1, the TAH count for this soil was extremely high; furthermore, Acidovorax Delafilldii and other phenanthrene degrading bacteria, have been isolated from this soil. Therefore, the experiment was repeated under conditions believed to supress the activity of PAH degrading bacteria. Specifically, the experiment was conducted at 4 °C and N_2 was used as the purge gas.

Desorption data from the $TNCLDN_2$ experiment is presented in Figure 4.17. Purge conditions used in this experiment are identical to those used in the TN soil experiment except that nitrogen is used as the purge gas and the apparatus is maintained at 4 °C to minimize biodegradation. The biphasic desorption pattern is not apparent with slightly less cummulative desorption of the three PAHs relative to the previous TN experiment. This is partly attributed to the effect of temperature on desorption rate. Biodegradation is minimized in this experiment as evidenced by the greater recovery of PAHs reported in Table 4.3. The standard error calculated by propagation of error was 19 % for all three compounds. The % recoveries reported in Table 4.3 were all within two standard errors of 100 %. After 500 hr, desorption ranges from 11 % for anthracene to 6 % for fluorene. In this experiment a desorption rate trend is not related to the sub-cooled liquid solubilities for the PAHs. Figure 4.18 shows the desorption rate for

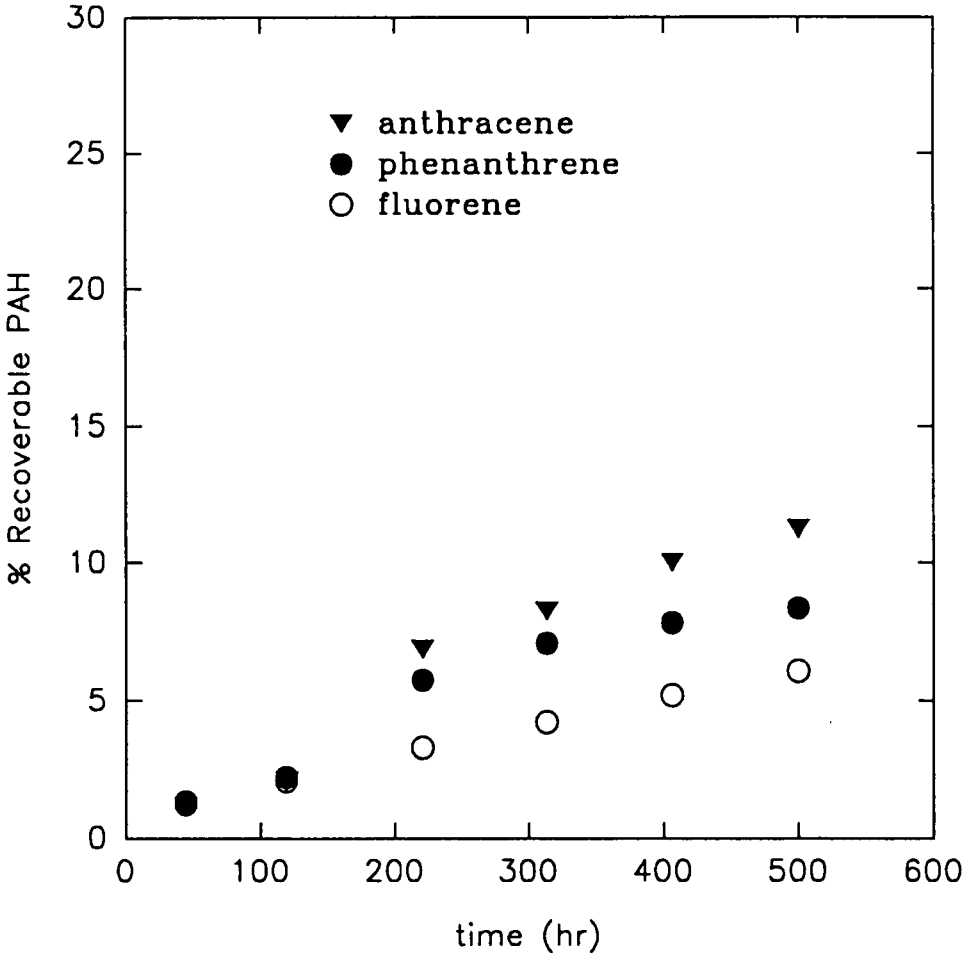

Figure 4.17 PAH Removals as a Function of Time in the TNCLDN2 Experiment

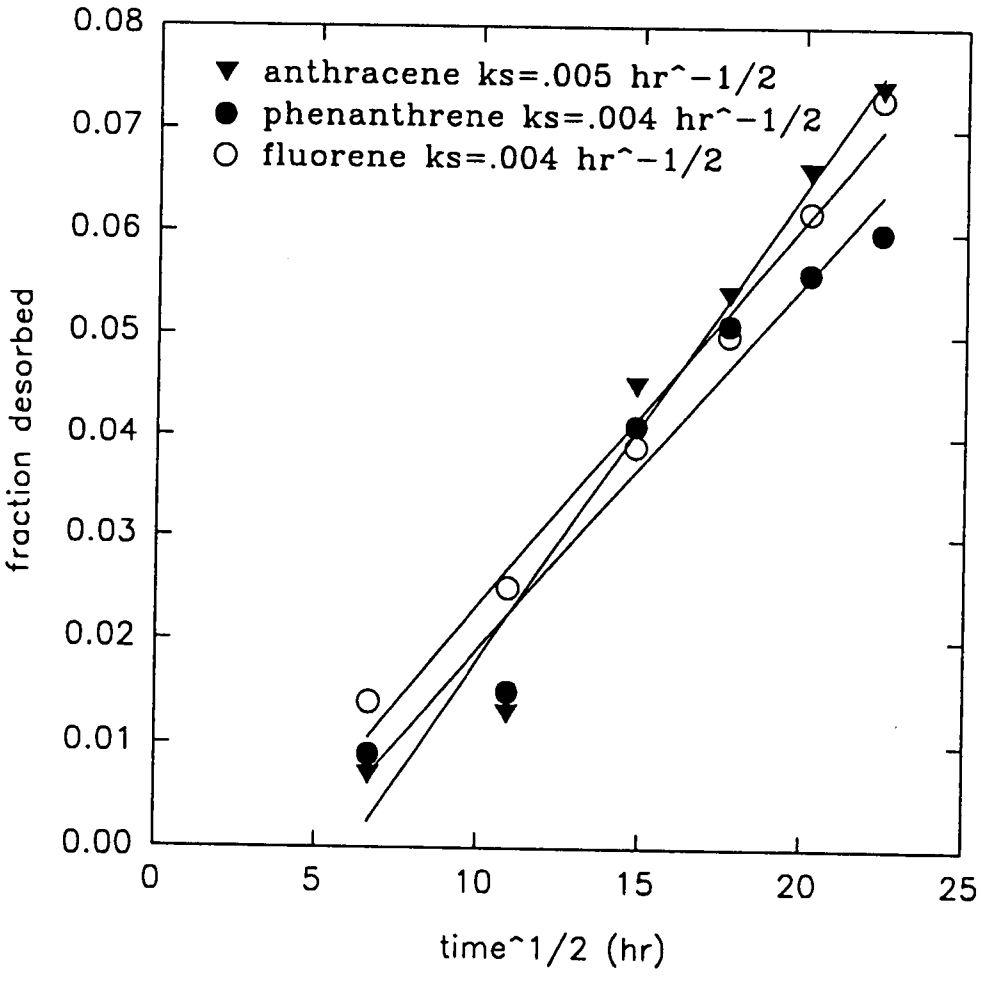

Figure 4.18 PAH Removals as a Function of the Square-Root of Time in the TNCLDN2 Experiment

each compound plotted against the square root of time. k_s's are very small, indicative of a slow desorption rate. Desorption rates are similar for the three PAHs, which has not been observed in previous experiments. The removal curves do not exhibit the "smooth" trend that has been apparent in other experiments. This may be attributed to fluctuations in the gas flow over time.

Table 4.6 summarizes k_s values for the desorption experiments as well as projections of the time required to achieve 99 % desorption. The projected time is the minimum time required to achieve 99 % desorption, and is based on the experimentally determined k_s value and Equation 4.3. The actual time is longer due to slope decrease as desorption proceeds. Decrease in slope can be attributed to exhaustion of source and decrease in concentration gradient. Times are not projected for ART experiments because they can be determined directly. The k_s values for artificially contaminated soils are much larger than k_s values for anthropogenically contaminated soils. However, the rate constants for the ARTGRI phenanthrene and the GRI phenanthrene are suprisingly close. This suggests that for this type of soil, contamination age is not a controlling parameter, and that the partitioning of PAH between the coal tar and the aqueous phase control the rate of desorption. Also, for the anthropogencially contaminated soils, the

Table 4.6 Summary of Desorption Rate Data

Experiment Name	k_s (hr^-1/2)	Projected Time for 99 % Desorption (years)
ART2d	ph = .112	n/a
ART20d	ph = .095	n/a
ART10m	ph = .062	n/a
ARTGRI	ph = .003	n/a
GRI	fl = .006 ph = .005 an = .003	fl = 3.1 ph = 4.5 an = 12.4
TN	fl = .011 ph = .004 an = .013	fl = 0.9 ph = 7.0 an = 0.7
TNCLDN2	fl = .004 ph = .004 an = .005	fl = 7.0 ph = 7.0 an = 4.5

range in rate constants is small between the three PAHs and two soil types.

Chapter 5

CONCLUSIONS

Desorption of PAHs from contaminanted soils can be studied effectively using gas purge. This method was used to quantify the desorption rate of specific PAHs from artificially and anthropogenically contaminated soil.

Desorption of PAHs from artificially contaminated soil shows a biphasic trend in which desorptioin occurs rapidly during the initial desorption period followed by slower desorption of the nonlabile fraction. Soils with contamination ages of 2 days, 20 days, and 300 days were used in the studies and show that resistance to desorption increases as contamination age increases. In other words, as contamination age increases, the easily desorbed fraction decreases relative to the nonlabile fraction. The rate of desorption decreases with increasing contamination age, as well. After approximately two weeks of purging, nearly 100 % of phenanthrene desorbed from soils contaminated for 2 days and 20 days; desorption from the 20-day soil was slightly slower. For the same desorption period, only 79 % of the removable phenanthrene desorbed from soil contaminated for 10 months. Desorption was further characterized using an infinite-source planar desorption model which yields a linear

relationship between the fraction desorbed and the square root of time. Diffusive mass transfer constants, k_s, obtained from this model range from 0.117 $hr^{-1/2}$ for the 2 day soil to 0.058 $^{-1/2}$ for the 10 month soil. The model describes desorption of the first 50 % of the phenanthrene from the 10-month soil and 60 % and 85 % for the 20-day and 2-day soils. This decrease for the 10 month soil can be explained by noting the assumptions of the model and the inward diffusion of phenanthrene as contamination age increases. The exhaustion of contaminant as desorption proceeds is also a factor in non-linear behavior. Overall, phenanthrene recoveries are excellent, within +/- 10 % of 100 %.

Approximately 5 % of the labeled phenanthrene added to GRI soil desorbed after a contamination age of 5 days. This extreme decrease in desorption rate, relative to ART soil, is due to the strong affinity of the GRI soil for phenanthrene. k_s was determined to be 0.002 $hr^{-1/2}$ for this soil. The model describes 100 % of the desorption over the given period. This is due to the small fraction of the contaminant that desorbs during the experiment. There is not an obvious biphasic desorption trend associated with this experiment. Most of the desorption is described by very slow desorption which immediately levels off and approaches 100 % asymptotically.

In the experiments conducted with anthropogenically

contaminated soils, desorption of fluorene, phenanthrene, and anthracene was studied. For the GRI soil, 30 % of fluorene, 9 % of phenanthrene, and 5 % of anthracene desorbed following 742 hr of purging. Fluorene exhibits more biphasic desorption than phenanthrene and anthracene. k_s values range from 0.003 to 0.006 $hr^{-1/2}$, which shows the slow desorption rate for these PAHs. 37 % of anthracene, 31 % of fluorene, and 11 % of phenanthrene desorb following 750 of continuous purging for the TN soil. Biphasic desorption is somewhat apparent in this experiment; however, desorption rate does not correlate with compound aqueous solubility. k_s values range from 0.013 to 0.004 $hr^{-1/2}$; a linear relationship between fraction desorbed and the square root of time describes the process over the entire desorption period. The TNCLDN2 experiment shows similar desorptive patterns with slightly less cummulative desorption for each compound. This is probably related to the lower diffusion coefficient associated with colder temperatures. k_s values remain in close agreement and range from 0.004 to 0.005 $hr^{-1/2}$ for the three compounds. Recovery of PAHs in these experiments are variable and can be explained by sample heterogeneity, experimental conditions, and analytical variance.

Overall, desorption rate of PAHs from soil is strongly related to contamination age and to the extent of contamination. If a previously clean soil is contaminated,

desorption rate is more a function of contamination age, with rate inversely proportional to contamination age. However, if a heavily contaminated soil is re-contaminated with fresh compound, the affinity of the soil for the compound makes contamination age a less important parameter. In this case, it is clear that ideal reversibility is not occurring due to the extremely fast uptake rate and very slow desorption rate following a relatively short contamination age. This study supports the occurrence of hysteresis for some systems. This is evidenced by considering the diffusive constants, k_s, for the ART experiments. As contamination age increases, k_s decreases or desorption rate decreases. While this work provides some data quantifying the desorption rates from anthropogenically contaminated soils, there remains a tremendous need for more work to be performed to investigate other factors (e.g. particle size and temperature) affecting the desorption rate.

List of References

List of References

1. Benefield, L.D., Judkins, J.F., and B.L. Weand, "Fundamentals of Surface and Colloidal Chemistry", in Process Chemistry for Water and Wastewater Treatment, Prentice-Hall, Inc., Englewood Cliffs, NJ, 192-202 (1982).

2. Brusseau, M.L., R.E. Jessup, and P.S.C. Rao, "Sorption Kinetics of Organic Chemicals: Evaluation of Gas-Purge and Miscible-Displacement Techniques", Environmental Science & Technology 24: 727-735 (1990).

3. Brusseau, M.L., R.E. Jessup, and P.S.C. Rao, "Nonequilibrium Sorption of Organic Chemicals: Elucidation of Rate-Limiting Processes", Environmental Science & Technology 25: 134-142 (1991).

4. Connaughton, D.F., J.R. Stedinger, L.W. Lion, and M.L. Shuler, "Description of Time-Varying Desorption Kinetics: Release of Napthalene from Contaminated Soils", Environmental Science &Technology 27: 2397-2403 (1993).

5. Cushey, M.A., and D.J. Morgan, "Biological Treatment of Soils Containing Manufactured Gas Plant Residues", Topical Report: Gas Research Institute, Chicago (June 1988-February 1990), Prepared by: Remediation Technologies, Inc., Pittsburgh (May 1990).

6. DiToro, D.M., and L.M. Horzempa, "Reversible and Resistant Components of PCB Adsorption-Desorption: Isotherms", Environmental Science &Technology 16: 594-602 (1982).

7. Edwards, D.A., R.G. Luthy, and Z. Liu, "Solubilization of Polycyclic Aromatic Hydrocarbons in Micellar Nonionic Surfactant Solutions", Environmental Science & Technology 25: 127-133 (1991).

8. ERT Project P-D215, Handbook on Manufactured Gas Plant Sites, Utility Solid Waste Activities Group Superfund Committee, Washington, Prepared by: Envr. Research and Tech., Inc. and Koppers Company, Inc., Pittsburgh.

9. Farrell, J., and M. Reinhard, "Desorption of Halogenated Organics from Model Solids, Sediments, and Soil Under Unsaturated Conditions. 1. Isotherms", Environmental Science &Technology 28: 53-62 (1994a).

10. Farrell, J., and M. Reinhard, "Desorption of Halogenated Organics from Model Solids, Sediments, and

Soil Under Unsaturated Conditions. 2. Kinetics", Environmental Science &Technology 28: 63-72 (1994b).

11. Gee, G.W., and J.W. Bauder, Particle size analysis in Methods of soil analysis. Part 1., 2nd edition. Klute, A (ed.) American Society of Agronomy, Madison, WI, p.383 (1986).

12. Harmon, T.C., and P.V. Roberts, "Measuring Contaminant Desorption Rate Using a Solvent Extraction Technique", Water Environment Federation Conference Paper, October (1993).

13. Harmon, T.C., and P.V. Roberts, "The Effect of Equilibration Time on Desorption Rate Measurements with Chlorinated Alkenes and Aquifer Particles", Environmental Progress, Vol. 13 No. 1, February (1994).

14. Kan, A.T., Gongmin Fu, and M.B. Tomson, "Adsorption/Desorption Hysteresis in Organic Pollutant and Soil/Sediment Interaction", Environmental Science & Technology 28: 859-867 (1994).

15. Karickhoff, S.W., "Semi-Empirical Estimation of Sorption of Hydrophobic Pollutants on Natural Sediments and Soils", Chemosphere Vol. 10, No. 8, 833-846 (1981).

16. Karickhoff, S.W., and K.R. Morris, "Sorption Dynamics of Hydrophobic Pollutants in Sediment Suspensions", Environmental Toxicology and Chemistry Vol. 4, 469-479 (1985).

17. Lane, W.F., and R.C. Loehr, "Estimating Equilibrium Aqueous Concentrations of Polynuclear Aromatic Hydrocarbons in Complex Mixtures", Environmental Science & Technology 26: 983-990 (1992).

18. Lee, L.S., M. Hagwell, J.J. Delfino, and P.S.C. Rao, "Partitioning of Polycyclic Aromatic Hydrocarbons from Diesel Fuel into Water", Environmental Science & Technology 26: 2104-2110 (1992a).

19. Lee, L.S., P.S.C. Rao, and I. Okuda, "Equilibrium Partitioning of Polycyclic Aromatic Hydrocarbons from Coal Tar into Water", Environmental Science & Technology 26: 2110-2115 (1992b).

20. Mackay, D., W.Y. Shiu, and R.P. Sutherland, "Determination of Air-Water Henry's Law Constants for Hydrophobic Pollutants", American Chemical Society Vol. 13 No. 3, March (1979).

21. Mackay, D., W.Y. Shiu, and K.C. Ma, Illustrated Handbook of Physical-Chemical Properties and Environmental Fate for Organic Chemicals Vol. 2, Polynuclear Aromatic Hydrocarbons, Polychlorinated Dioxins, and Dibenzo Furans, Lewis Publishers, Michigan, (1992).

22. Mackay, D., and W.Y. Shiu, "A Critical Review of Henry's Law Constants for Chemicals of Environmental Interest", J. Phys. Chem. Ref. Data Vol. 10, No. 4, 1175-1191 (1981).

23. Means, J.C., S.G. Wood, J.J. Hassett, and W.L. Banwart, "Sorption of Polynuclear Aromatic Hydrocarbons by Sediments and Soils", Environmental Science & Technology 14: 1524-1528 (1980).

24. Miller, C.T., and J.A. Pedit, "Use of a Reactive Surface-Diffusion Model to Describe Apparent Sorption-Desorption Hysteresis and Abiotic Degradation of Lindane in a Subsurface Material", Environmental Science & Technology 26: 1417-1427 (1992).

25. Mueller, J.G., P.J. Chapman, and P.H. Pritchard, "Creosote-Contaminated sites", Environmental Science & Technology Vol. 23, No. 10, 1197-1201 (1989).

26. Murphy, Environmental Science and Technology 24, 1507 (1990).

27. Oliver, B.G., "Desorption of Chlorinated Hydrocarbons from Spiked and Anthropogenically Contaminated Sediments", Chemosphere Vol. 14, No. 8, 1087-1106 (1985).

28. Pavlostathis, S.G., and K. Jaigal, "Desorptive Behavior of Trichloroethylene in Contaminated Soil", Environmental Science & Technology 25: 274-279 (1991).

29. Pavlostathis, S.G., and G.N. Mathavan, "Desorption Kinetics of Selected Volatile Organic Compounds from Field Contaminated Soils", Environmental Science & Technology 26: 532-538 (1992).

30. Schwarzenbach, R.P., P.M. Gschwend, and D.M. Imboden, Environmental Organic Chemistry, John Wiley & Sons, Inc., New York (1993).

31. Wu, S., and P.M. Gschwend, "Sorption Kinetics of Hydrophobic Organic Compounds to Natural Sediments and Soils", Environmental Science & Technology 20: 717-725 (1986).

32. Young, D.F., and W.P. Ball, "A Priori Simulation of Tetrachloroethene Transport Through Aquifer Material Using an Intraparticle Diffusion Model", Environmental Progress, Vol. 13, No. 1, 9-19 (February 1994).

Appendix

Appendix A - Sample Chromatograms

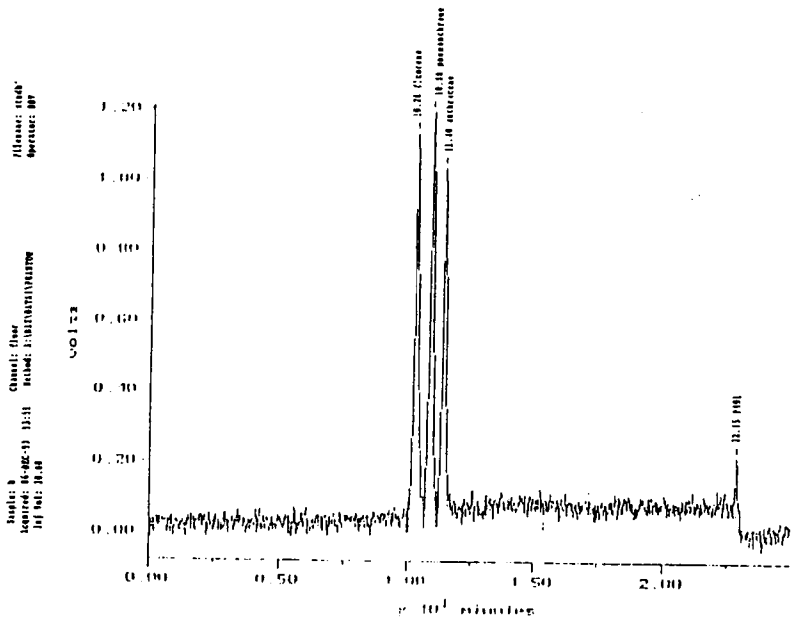

Figure A.1 Chromatogram for PAH Standards

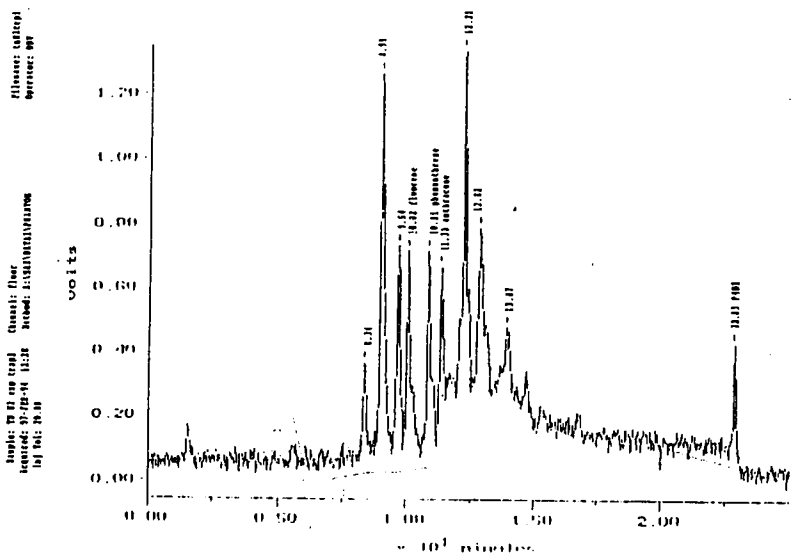

Figure A.2 Chromatogram for PAH Extraction from Soil

Appendix B - Progegation of Error

standard error for soxhlet extraction = 13 %

standard error for final extraction = 15 %

standard error for summation of traps = 11.5 %

standard error approximations taken from soxhlet extraction triplication data, estimated final extraction error, and solution purge experimental recoveries

mass recovery = (summation traps + final extraction)/soxhlet

if a value, v, is dependant on three independent variables, x, y, z, then:

$$\partial_v = \sqrt{\left(\frac{\partial v}{\partial x}\times\partial_x\right)^2+\left(\frac{\partial v}{\partial y}\times\partial_y\right)^2+\left(\frac{\partial v}{\partial z}\times\partial_z\right)^2}$$

derived equation for overall standard error in recovery:

$$= \left((.115*f_{desorb})^2+(0.15(1-f_{desorb}))^2+(.13)^2\right)^{1/2}$$

Expt. Name	Standard Error (%)
TN	fl - 17 ph - 19 an - 17
GRI	fl - 15 ph - 19 an - 19
TNCLDN2	fl - 19 ph - 19 an - 19

Vita

James Reed Stanley was born in Abingdon, Virginia on February 14, 1969. He attended Abingdon Elementary School and graduated from Abingdon High School in 1987. In August 1987 he entered The University of Tennessee, Knoxville and received a Bachelor of Science degree in Chemistry in August 1991. He reentered The University of Tennessee, Knoxville in August 1991 and received a Master of Science degree in Environmental Engineering in December 1994.